Development of Liquid-Phase Agitated Reactors: Synthesis, Simulation, and Scaleup

Ketan D. Samant and Ka M. Ng
Dept. of Chemical Engineering, University of Massachusetts, Amherst, MA 01003

A systematic procedure is formulated for the development of liquid-phase agitated reactors. The procedure has three components: synthesis, simulation, and scaleup. Synthesis leads the user to the reactor geometry, agitator type and speed, number and location of feed addition ports, feed addition or residence time, and heat-transfer policy that would achieve the desired performance objectives. It is based on an analysis of the interplay of reaction and mixing at various length scales, and a knowledge base of the capacities of heat-transfer equipment. Simulation assesses the performance of the reactors thus synthesized, taking into account detailed flow properties obtained through computational fluid dynamic simulations, experimental data, or a combination of both. Scaleup provides fundamentally based scaleup rules for direct development of these reactors from laboratory scale to production scale. A comparison of these derived scaleup rules with published empirical rules reveals the underlying physics, applicability, and limitations of these empirical rules. Three examples are presented to illustrate the use of this procedure.

Introduction

Production of specialty chemicals typically involves multistep reactions. The volume of production is modest in comparison to the commodity chemical industry. Semibatch and continuous agitated reactors are often used because of their relatively simple construction and easy operation. In the initial development phase of these processes, the chemist carries out experiments in laboratory-scale reactors of size around 1 to 10 L. The primary objective is to determine the yield, selectivity of desired product, and level of impurity byproducts. If these performance measures of the candidate reaction are acceptable for commercial exploitation, additional work is carried out to design a full-scale reactor with suitable operating conditions. It is, however, not uncommon to find that a reaction attractive on the laboratory scale does not provide the desired performance on the production scale. The most common cause of this discrepancy is an incomplete understanding and improper treatment of the interplay of mixing and complex reaction schemes with one or more fast reaction steps.

Correspondence concerning this article should be addressed to K. M. Ng.

The importance of turbulent reactive mixing has long been recognized (Toor, 1962, 1969; Ottino, 1981; Chella and Ottino, 1984; Baldyga and Pohorecki, 1995). A number of studies involving modeling techniques of varying degrees of complexities such as direct numerical simulations (Leonard and Hill, 1988; Chakrabarti et al., 1995), probability density function methods (Fox, 1992; Pipino and Fox, 1994), phenomenological models like the Engulfment-Deformation-Diffusion (EDD) model (Baldyga and Bourne, 1984a); the Interaction by Exchange with Mean (IEM) model (David and Villermaux, 1987; Villermaux and Falk, 1994), and cell balance methods such as the network of zones model (Mann et al., 1995) can be found in the literature. Turbulent reactive mixing in liquid-phase agitated reactors has most commonly been studied with the aid of phenomenological mixing models (Baldyga and Bourne, 1984b, 1989; David and Villermaux, 1987; Bourne and Yu, 1994; and so on). While these fundamental studies demonstrate the effects of mixing on fast chemical reactions, a systematic procedure for the development of agitated reactors for given performance objectives is not available. In this article, a procedure, which identifies

ideal reactor attributes and operating conditions, simulates the reactor performance and suggests rules for direct development from laboratory to production scale is presented.

The development procedure is divided into three components. The first is a three-step reactor synthesis procedure. In Step 1, the reactor performance in various operating regimes is estimated and the operating regime in which the desired reactor performance can be obtained is identified. In Step 2, reactor attributes such as reactor geometry, impeller type and geometry, number and location of feed addition ports and operating conditions such as feed addition time and agitator operating speed are chosen so as to be in the desired operating regime as far as possible. In Step 3 of the synthesis procedure, heat-transfer equipment is added to the reactor thus synthesized. The second component deals with simulations which evaluate the performance of the proposed reactor with realistic flow fields obtained from CFD simulations or experimental data. The third component consists of fundamentally derived scale-up rules, which allow direct development of agitated reactors from the laboratory scale to the production scale. The development procedure is illustrated with three representative examples.

Synthesis of Single-Phase Agitated Reactors

The objective here is to develop an efficient and flexible procedure to select reactor attributes and operating conditions for the system on hand by properly accounting for the interplay of mixing and chemical reactions and the heat-transfer requirements. Some information about the system under consideration is needed for this purpose. Therefore, we begin with a discussion of the required input information, the phenomenological model equations for mixing and chemical reactions, and classification of reactor operation into various operating regimes.

Input information

The input information is classified into three categories, viz., information about the reactions, the components, and the process (Table 1). The reaction and component information includes the reaction stoichiometry, rate expressions, kinetic parameters such as rate constants, activation energies, and heats of reactions, and physical properties of components such as densities, viscosities, and molecular weights. This information is typically obtained via physical property databases and experimentation during the initial phase of development. The process information includes the performance objectives, the mode of operation (batch, semibatch, or continuous), total production time, reactor size to be used, and any other operating constraints. Typically, these decisions are made on the basis of the nature of the reaction network, the products, the production rate, availability of existing equipment, safety and environmental concerns, and so on (Levenspiel, 1972; Douglas, 1988; Biegler et al., 1997).

Table 1. Input Information Required for Development of Agitated Reactors

Information about the reactions
Reaction stoichiometry and rate expressions
Reaction rate constants and activation energies
Heats of reaction
Information about the components
Information about purity of reactants
Physical properties of all components (ρ, ν, λ, C_p, M, etc.)
Information about the process
Performance objectives
Mode of operation
Production time
Reactor size desired and available
Other operating constraints (equipment limitations, availability of utilities, safety concerns such as prevention of excessive heat evolution, etc.)

Phenomenological description of turbulent reactive mixing in agitated reactors

In single liquid-phase agitated reactors operating under turbulent flow conditions, widely different length scales are involved in the mixing process. The microscale involves viscous-convective deformation of fluid elements which accelerates molecular-scale diffusion and chemical reaction. The mesoscale refers to the inertial-convective disintegration of large eddies which leads to the reduction in the scale of the concentration fluctuations (Baldyga and Rohani, 1987). The macroscale involves convection of fluid elements throughout the reactor and is of the order of the reactor itself. The course of chemical reactions which are molecular events is affected directly by micromixing. Mesomixing and macromixing have only an indirect effect as they determine the environment for micromixing and convey the fluid elements undergoing micromixing through regions of varying turbulence properties.

It is difficult to solve a fluid dynamical model for an agitated reactor that includes a complete description of all three mixing length scales. A more convenient method is to use phenomenological models for micro- and mesomixing, and fluid dynamical models or experimental observations for macroscale flow. In this article, we use the widely used Engulfment-Deformation-Diffusion (EDD) model (Baldyga and Bourne, 1984a) which captures the key physical processes contributing to turbulent mixing. The development and application of this model can be traced through Baldyga and Bourne (1984a,b, 1988, 1989, 1992), Baldyga et al. (1997), and Bourne and Yu (1994). Here, for the sake of brevity, we discuss only the important equations and the characteristic mixing time scales relevant to our reactor development procedure.

Discretized feed addition is used to model semibatch and continuous operations. In other words, despite the fact that the feed flows continuously, it is treated as a series of discrete feed elements entering the reactor sequentially. Each incoming fluid element is rolled up by turbulent vorticity thereby creating multiple layers or slabs of fresh liquid and liquid already in the reactor. This incorporation of liquid from the environment into the deforming vortices is called *engulfment*. The vortices thus formed undergo *deformation* thereby reducing the scale of segregation by elongation and shrinkage of the embedded slabs. *Diffusion* and chemical reactions take place within these deforming slabs until the vortices die out, at which point a fresh burst of vorticity sets the fluid into motion again. For liquids, engulfment is the rate controlling

process ($Sc < 4{,}000$). Thus, the rate of growth of the volume of the micromixed region can be written as (Baldyga and Bourne, 1989)

$$\frac{dV}{dt} = EV; \qquad V(t=0) = V_o \tag{1}$$

where the engulfment rate E (1/s) is defined as

$$E = \frac{\ln 2}{12(\nu/\epsilon)^{1/2}} = 0.058\left(\frac{\epsilon}{\nu}\right)^{1/2} \tag{2}$$

Also, the characteristic micromixing time scale is given by

$$t_m = E^{-1} = \frac{12}{\ln 2}\left(\frac{\nu}{\epsilon}\right)^{1/2} \tag{3}$$

Engulfment may not always involve interaction of the feed fluid element with its environment. Engulfment within the fluid elements (self-engulfment) does not contribute to the growth of the volume of the micromixed region. Equation 1 can be corrected for self-engulfment as

$$\frac{dV}{dt} = EVf; \qquad V(t=0) = V_o \tag{4}$$

where the self-engulfment factor f may be written using the model of mesomixing by eddy disintegration as (Baldyga et al., 1997)

$$f = 1 - \frac{V}{V_o}\exp\left(\frac{-t}{t_s}\right) \tag{5}$$

Here, t_s is the characteristic time scale of mesomixing (s) which can be expressed for agitated reactors as

$$t_s = 2\left(\frac{Q_f}{\pi u \epsilon n_f}\right)^{1/3} \tag{6}$$

In this description of mixing, the macromixing process is characterized by the macroscopic flow field and the rate of turbulent energy dissipation per unit mass within the reactor. Circulation time (t_c) (s) defined as

$$t_c = (\pi/4)\, N_q^{-1} d^{-3} D^3 N^{-1} \tag{7}$$

is thus chosen as the characteristic macromixing time scale.

Now, for a system of c components and r reactions, the rate of change of composition of component i in the growing fluid elements can be written as (Appendix)

$$\frac{dx_i}{dt} = \frac{1}{t_m}\frac{M_x}{M_y}(y_i - x_i)\left[1 - \frac{V}{V_o}\exp\left(\frac{-t}{t_s}\right)\right] + \sum_{j=1}^{r}(\nu_{i,j} - x_i\nu_{\mathrm{TOT},j})R_j; \quad x_i(t=0) = x_i^F \tag{8}$$

Here, x and y are the compositions of the fluid element and its environment, respectively, x^F is the feed composition. $\nu_{i,j}$ is the stoichiometric coefficient of component i in reaction j and $\nu_{\mathrm{TOT},j}$ is the algebraic sum of stoichiometric coefficients of all components for reaction j. M_x and M_y are average molecular weights (kg/mol) of the fluid elements and the environment, respectively

$$M_x = \sum_{i=1}^{c} M_i x_i \tag{9a}$$

$$M_y = \sum_{i=1}^{c} M_i y_i \tag{9b}$$

It should be noted that in these equations, the macroscale is not accounted for explicitly. Instead, the macroscale properties are calculated separately and the environment composition is assumed to be uniform. This may not give very accurate results when the volumetric feed flow rate is comparable to the volumetric flow through the reactor; that is, when the characteristic macromixing time (t_c) is comparable with the feed addition time (t_c) (s) for semibatch operation or with average residence time ($\bar{t}$) (s) for continuous operation.

With the above model equations and characteristic time scales for mixing at various length scales, we can now identify various regimes of reactor operation. This is done on the basis of the relative rates of the mixing processes at various length scales and of chemical reactions.

Operating regimes

The rate of reaction j per mole of reacting mixture of composition x can be written as

$$R_j = k_j r_j(x) = \frac{1}{t_r}\frac{k_j}{k_{\max}} r_j(x) \tag{10}$$

where t_r the characteristic time (s) for reaction is given by

$$t_r = \frac{1}{k_{\max}} = \frac{1}{\max_j(k_j)} \tag{11}$$

This definition reflects our desire to compare the rates of the mixing processes to the rate of the fastest reaction. To facilitate the classification of reactor operation into various mixing regimes, let us define the following dimensionless numbers

$$Da_m = \frac{t_m}{t_r} = \frac{\text{Characteristic Micromixing Time}}{\text{Characteristic Reaction Time}} \tag{12a}$$

$$Da_s = \frac{t_s}{t_r} = \frac{\text{Characteristic Mesomixing Time}}{\text{Characteristic Reaction Time}} \tag{12b}$$

$$Q = \frac{t_m}{t_s} = \frac{Da_m}{Da_s} = \frac{\text{Characteristic Micromixing Time}}{\text{Characteristic Mesomixing Time}} \tag{12c}$$

The Damköhler numbers for micromixing (Da_m) and mesomixing (Da_s) compare the characteristic time for micromix-

ing and mesomixing, respectively, to the characteristic time for reaction. The mixing index (Q) compares the characteristic time scales of micro- and mesomixing. Let us cast Eq. 4, which represents the volumetric expansion of micromixed fluid elements, into dimensionless form using $\theta = t/t_m$ and $\varphi = V/V_o$.

$$\frac{d\varphi}{d\theta} = \varphi[1 - \varphi \exp(-Q\theta)]; \qquad \varphi(\theta = 0) = 1 \qquad (13)$$

For $Q \gg 1$, the term within the square brackets tends to unity. This indicates that the self-engulfment is negligible and mesomixing is not important. Here $t_m \gg t_s$ and micromixing is the controlling mechanism. As Q decreases below unity, self-engulfment and, hence, mesomixing becomes increasingly significant. Mesomixing can be said to be controlling for $Q < 1$ or $t_m < t_s$. Although macromixing is not accounted for explicitly, it can be said to be controlling when the macromixing time scale (t_c) becomes comparable to the time scale of feed addition (t_f or $\bar{t}$). As will be shown in Step 2 of the synthesis procedure (after Eq. 25), this occurs as Q decreases significantly below unity.

Similarly, casting Eq. 8 into dimensionless form by using $\theta = t/t_r$ and $\varphi = V/V_o$, we get

$$\frac{dx_i}{d\theta} = \frac{1}{Da_m}\frac{M_x}{M_y}(y_i - x_i)\left[1 - \varphi \exp\left(\frac{-Q\theta}{Da_m}\right)\right] + \sum_{j=1}^{r}(\varphi_{i,j} - x_i\varphi_{\mathrm{TOT},j})\frac{k_j}{k_{\max}}r_j(x); \quad x_i(\theta = 0) = x_i^F \qquad (14)$$

The lefthand side and the second term on the righthand side of this dimensionless equation are of order unity. Hence, the first term on the righthand side should also scale as unity. For $Da_m \ll 1$, this would be true if

$$\text{for } Q > 1, \quad (y_i - x_i) \approx 0 \qquad (15a)$$

$$\text{for } Q < 1, \quad (y_i - x_i)\left[1 - \varphi \exp\left(\frac{-Q\theta}{Da_m}\right)\right] \approx 0 \qquad (15b)$$

Equation 15a indicates that for $Q > 1$, $Da_m \ll 1$, the environment composition is the same as the composition of the micromixed fluid elements. Hence, under these conditions, the reactor contents are perfectly mixed. From Eq. 15b, we can draw the same conclusions ($y_i \approx x_i, \forall i$) if the term within the square brackets is of order unity, that is, if $Q/Da_m \gg 1$ or $Da_s \ll 1$. Hence, combining these observations, perfect mixing can be assumed for $Q > 1$, $Da_m \ll 1$ and $Q < 1$, $Da_s \ll 1$, that is, when the time scale for the controlling mixing mechanism is much smaller than the time scale for reaction.

These operating regimes are depicted in Figure 1. Perfectly mixed regime is bounded by $Q > 1$, $Da_m \leq 0.01$ and $Q < 1$, $Da_s \leq 0.01$ and is indicated by the unshaded region. The micromixing controlled regime corresponds to $Q > 1$ (region shaded with patterns) and the meso- and macromixing controlled regime corresponds to $Q < 1$ (region shaded uniformly). As noted earlier, macromixing becomes increasingly significant as the mixing index decreases. The boundaries of these regimes are not sharp. The shading convention for micro- and mesomixing controlled regimes is followed throughout the rest of the article.

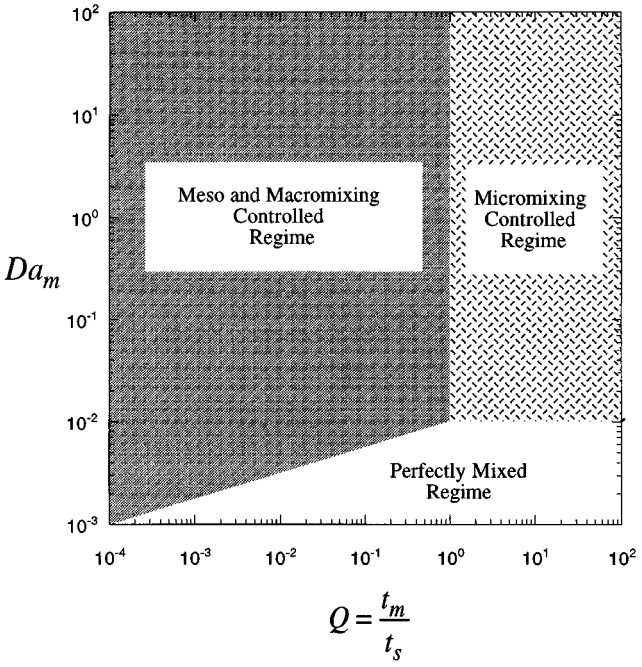

Figure 1. Operating regimes as functions of Damköhler number for micromixing (Da_m) and mixing index (Q).

Synthesis procedure

In Step 1 of the synthesis procedure, we examine the reactor performance in various operating regimes. The desired operating regime and the corresponding values for the Damköhler numbers and mixing index are identified. We then relate the dimensionless numbers to reactor attributes and operating conditions and use these relationships as the basis for appropriately choosing these attributes and operating conditions in Step 2. Finally, in Step 3, a suitable heat-transfer policy is chosen based on the heat-transfer requirements and available equipment. Steps 1 and 2 of the procedure are valid for liquid-phase reactors with a uniform feed composition.

The various steps involved in the procedure are discussed below with the help of an example (referred to as Example I). This example involves a four-component system of consecutive-competing reactions given by

$$\begin{aligned} A + B &\rightarrow C \\ B + C &\rightarrow D \end{aligned} \qquad (16)$$

This situation corresponds to the classical reaction scheme that has been used extensively in modeling (Baldyga and Bourne, 1984b, 1992) and experimental (Bourne and Dell'Ava, 1987; Bourne and Hilber, 1990; Tipnis et al., 1994) studies. C is the desired product that undergoes a side reaction with one of the reactants B to produce the undesired product D.

Table 2. Input Information for Example I

Information about the reactions	
$A + B \rightarrow C;$ $\quad R_1 = k_1 x_A x_B$	
$B + C \rightarrow D;$ $\quad R_2 = k_2 x_B x_C$	
$k_1 = k_2 = 4.327 \times 10^9 \exp(-5{,}000/TCK)\ \mathrm{s}^{-1}$	
$k_1 = k_2 = 250\ \mathrm{s}^{-1}$ @ $T = 300$ K	
$\Delta H = -2.2 \times 10^5$ J/mol·B reacted	
Information about the components with pure A and B as reactants	
$\rho = 10^3$ kg/m^3	$M_A = 1{,}000$ g/mol
$\nu = 2 \times 10^{-6}$ m^2/s	$M_B = 60$ g/mol
$C_p = 4.18 \times 10^3$ J/kg·K	$M_C = 1{,}060$ g/mol
$\lambda = 0.614$ W/m·K	$M_D = 1{,}120$ g/mol
Information about the process	
Semibatch addition of B	
Isothermal operation at 300 K	
Reactor size = 1,000 L ($D = 1.08$ m)	
Max. production time for the reactor (t_p) = 6,000 s	
Max. power input/unit vol. (P_{max}) = 2,000 W/m^3	

The performance objective is to maximize the product distribution defined as

$$\text{Product Distribution} = \frac{C \text{ Produced}}{B \text{ Reacted}} \tag{17}$$

B is added in semibatch mode to the reactor containing A. Other input information for this example is listed in Table 2.

Step 1: Estimation of Reactor Performance in Various Operating Regimes. Reactor performance in various operating regimes is estimated by solving Eq. 14 for different values of Damköhler numbers and mixing index. The values of these dimensionless numbers are assumed constant throughout the reactor. It should be noted that in reality, these values are different at different locations within a reactor. Due to these spatial variations, the actual reactor performance is going to be different than that estimated using constant values of dimensionless numbers. However, for rigorous performance estimation, local values of the rate of dissipation of turbulent kinetic energy per unit mass (ϵ) (m^2/s^3) and fluid velocity (u) (m/s) must be known. These values depend on the reactor attributes and operating conditions. At this stage, our aim is to choose the most suitable combination of reactor attributes and operating conditions from among a number of possible combinations. Detailed knowledge of local values of ϵ and u for all these combinations will require enormous development time and cost. Hence, the use of constant values of the dimensionless numbers is a very convenient and practical approach. Once the reactor attributes and operating conditions are chosen, rigorous performance evaluation may be done, if deemed necessary, by using the simulation methods discussed in the second component of the development procedure. This division of tasks between the synthesis and simulation components makes the procedure flexible and efficient.

Performance evaluation has to be done individually for every reaction system to be considered. However, the following general observations can be made. For a given value of Da_m, the reactor performance does not change in the micromixing controlled regime with changing values of Q. This is due to the fact that in this regime, the self-engulfment factor is close to unity thus leaving Eq. 14 unaffected by changes in Q. However, as Q decreases below unity, mesomixing effects become increasingly significant and the performance changes with changing values of Q. Also, in the perfectly mixed regime, $Q > 1$, $Da_m \ll 1$ or $Q < 1$, $Da_s \ll 1$, the performance is naturally not affected by the dimensionless numbers.

Step 1 for Example I. The reactor performance in various operating regimes is shown in Figure 2. Figure 2a shows the product distribution as a function of the mixing index for different values of Damköhler number for micromixing. For a given value of Da_m, the product distribution has its highest value in the micromixing controlled regime. As Q decreases below unity, self-engulfment decreases the product distribution for this example, as reactant B which takes part in the

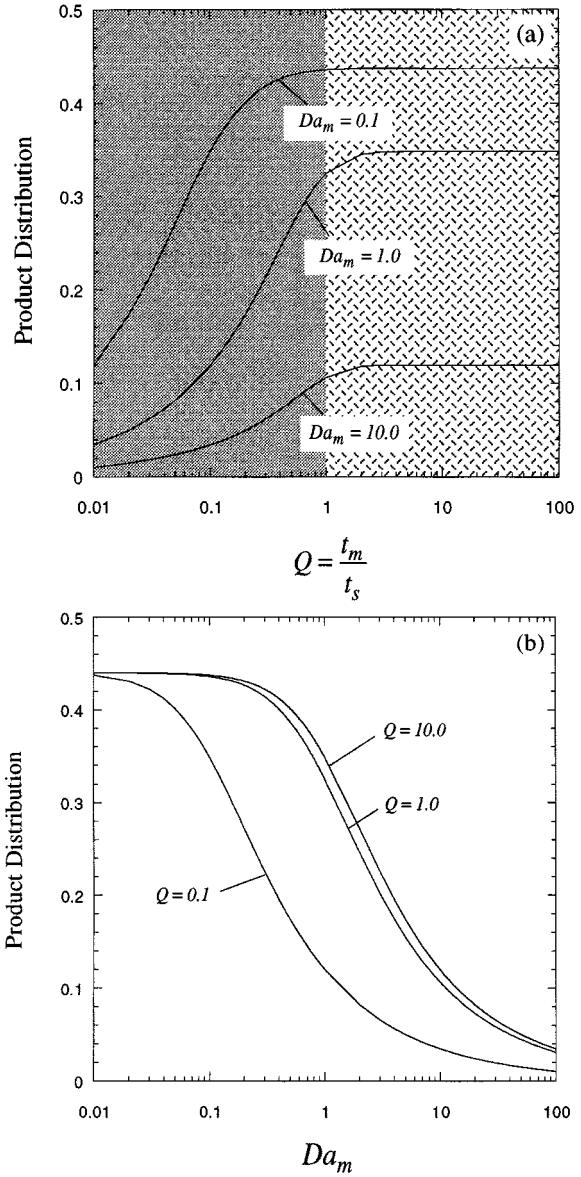

Figure 2. Reactor performance in various operating regimes for Example I.

(a) Product distribution as a function of mixing index; (b) product distribution as a function of Damköhler number for micromixing.

undesired reaction is added in semibatch fashion. Also, for a given value of Q, the product distribution is higher for lower values of Da_m. This can be seen easily from Figure 2b, which shows the variation of product distribution with Da_m for different values of Q. Clearly, the product distribution has its highest value in the perfectly mixed regime ($Q > 1$, $Da_m \ll 1$ or $Q < 1$, $Da_s \ll 1$) and decreases as the mixing processes become more significant.

Therefore, we would like to operate, if possible, in the perfectly mixed regime. This may not be feasible, as is the case with most reaction schemes that involve one or more fast reactions. In such a case we would like to operate in the micromixing controlled regime with as low a value of Da_m as possible.

Step 2: Selection of Reactor Attributes and Operating Conditions. Operating regimes can be expressed as functions of reactor attributes and operating conditions by relating the Damköhler numbers and the mixing index to them. The various parameters in Eqs. 3 and 6 for t_m and t_s, respectively, can be expressed using standard equations as

$$Q_f = V_R/at_f; \quad \text{for semibatch operation}$$
$$= V_R/t; \quad \text{for continuous operation} \tag{18a}$$

$$\epsilon_{\text{avg}} = N_p d^5 N^3/V_R \tag{18b}$$

$$u_{\text{avg}} = 2^{1/2} N_p^{1/2} N_q^{-1/2} Nd \tag{18c}$$

$$V_R = (\pi/4) D^3 \tag{18d}$$

Note that as the dimensionless numbers are assumed to be constant throughout the reactor, average values of ϵ and u are used to evaluate them. In what follows, we will focus our attention on semibatch operation. It is a simple matter to extend the analysis to include continuous operation.

Using Eqs. 18a to 18d, we can write t_m and t_s as

$$t_m = 6(\ln 2)^{-1} \pi^{1/2} N_p^{-1/2} N_{Re}^{-1/2} \xi^{-3/2} N^{-1} \tag{19a}$$

$$t_s = 2^{-1/2} \pi^{1/3} a^{-1/3} N_p^{-1/2} N_q^{1/6} \xi^{-2} \left(N^4 t_f n_f \right)^{-1/3} \tag{19b}$$

and the Damköhler numbers and the mixing index as

$$Da_m = 6(\ln 2)^{-1} \pi^{1/2} N_p^{-1/2} N_{Re}^{-1/2} \xi^{-3/2} N^{-1} k_{\max} \tag{20a}$$

$$Da_s = 2^{-1/2} \pi^{1/3} a^{-1/3} N_p^{-1/2} N_q^{1/6} \xi^{-2} \left(N^4 t_f n_f \right)^{-1/3} k_{\max} \tag{20b}$$

$$Q = 6(\ln 2)^{-1} 2^{1/2} \pi^{1/6} a^{1/3} N_{Re}^{-1/2} N_q^{-1/6} \xi^{1/2} \left(N^4 t_f n_f \right)^{1/3} \tag{20c}$$

where

$$N_{Re} = Nd^2 \nu^{-1} \tag{21a}$$

and

$$\xi = dD^{-1} \tag{21b}$$

Equations 20a to 20c relate the operating regimes directly or indirectly to reactor attributes, such as geometry and agitator type (ξ, N_p, N_q), number of feed ports (n_f), and operating conditions such as agitator speed (N, N_{Re}), and feed addition time (t_f), and form the basis for their selection.

The power input per unit volume (P) (W/m^3) is given by

$$P = (4/\pi) N_p N^3 D^2 \xi^5 \rho \tag{22}$$

Using Eq. 22, the dimensionless numbers can also be expressed as functions of P as

$$Da_m = \frac{12}{\ln 2} k_{\max} \left(\frac{\nu \rho}{P} \right)^{1/2} \tag{23a}$$

$$Da_s = 2^{7/18} \pi^{-1/9} \frac{k_{\max} N_q^{1/6} \xi^{2/9} D^{8/9}}{\left(at_f n_f \right)^{1/3} N_p^{1/18}} \left(\frac{\rho}{P} \right)^{4/9} \tag{23b}$$

$$Q = \frac{12 \pi^{1/9}}{2^{7/18} \ln 2} \frac{\left(at_f n_f \right)^{1/3} \nu^{1/2}}{N_q^{1/6} \xi^{2/9} D^{8/9}} \left(\frac{\rho N_p}{P} \right)^{1/18} \tag{23c}$$

The characteristic macromixing time is given by Eq. 7. This time scale can be compared with the time of feed addition by the ratio

$$\frac{t_c}{t_f n_f} = \left(\frac{\pi}{4} \right) N_q^{-1} \xi^{-3} N^{-1} t_f^{-1} n_f^{-1} \tag{24}$$

Using Eq. 20c, this ratio can be expressed as

$$\frac{t_c}{t_f n_f} = \left(\frac{6 \pi^{1/2}}{2^{1/6} \ln 2} \right)^3 a N_q^{-3/2} N_{Re}^{-3/2} \xi^{-3/2} Q^{-3} \tag{25}$$

Thus, as Q decreases, this ratio increases and, for very low values of Q, approaches unity. Here, the feed addition time becomes comparable to the macromixing time scale. This is the reason why we move into the macromixing controlled regime for very low values of Q as mentioned earlier.

Before we proceed to demonstrate this step for Example 1, a few comments about reactor attributes are in order. As mentioned before, a great variety of agitator types (axial flow such as pitched blade turbines, and radial flow such as flat blade turbines), reactor shapes (flat bottom, round bottom, and so on) and reactor geometries (number and size of baffles, clearance from tank bottom, agitator diameter relative to tank diameter, and so on) can be used. Each combination has a value of power number (N_p) and pumping number (N_q) associated with it. These are the values that we need to relate the reactor attributes to the reactor performance. Thus, many different combinations of agitator types and reactor geometries can be considered provided the values of N_p and N_q are available. These values are typically estimated from literature correlations or from simple in-house experiments. Here, we consider six most commonly used agitator types and corresponding standard reactor geometries (Table 3). Turbulent flow power and pumping numbers for these configurations are listed in Table 4 along with the sources of this information. Additional agitator types, reactor geometries, and use of multiple impellers can easily be included.

Table 3. Agitator Types and Reactor Geometries Under Consideration

Config.	Agitator Type	Principal Flow Pattern	Important Geometric Details
A1	Marine propeller	Axial	Flat bottom with 4 baffles $n_b = 3,\ \alpha = 25°,\ h/d = 1.5,\ d/D = 1/3,$ $H/D = 1,\ w_b/D = 1/12$
A2	Pitched blade turbine	Axial	Flat bottom with 4 baffles $n_b = 6,\ \alpha = 45°,\ h/d = 1,\ d/D = 1/3,$ $w/d = 1/8,\ H/D = 1,\ w_b/D = 1/12$
R1	Flat blade disc (Rushton) turbine	Radial	Flat bottom with 4 baffles $n_b = 6,\ h/d = 1,\ d/D = 1/3,\ w/d = 1/5$ $H/D = 1,\ w_b/D = 1/12$
R2	Flat blade turbine	Radial	Flat bottom with 4 baffles $n_b = 6,\ h/d = 1,\ d/D = 1/3,\ w/d = 1/5,$ $H/D = 1,\ w_b/D = 1/12$
R3	Curved blade turbine	Radial	Flat bottom with 4 baffles $n_b = 6,\ h/d = 1,\ d/D = 1/3,\ w/d = 1/8,$ $H/D = 1,\ w_b/D = 1/12$
R4	Retreating blade (Pfaudler) impeller	Radial	Flat bottom with 4 baffles $n_b = 3,\ h/d = 1/4,\ d/D = 1/2,\ w/d = 1/10,$ $H/D = 1,\ w_b/D = 1/12$

d = agitator dia. h = clearance off tank bottom n_b = no. of blades w_b = baffle width
D = reactor dia. H = reactor height w = agitator blade width α = blade pitch

Step 2 for Example I: Feed Addition Time. The production time (t_p) (s) gives the upper bound on the feed addition time. The production time constraint typically arises out of the need to achieve a desired production target. The feed addition time should also be much longer than the circulation time. Thus, we can write

$$Ct_c \le n_f t_f \le n_f t_p \tag{26}$$

Typically, C ranges from 10 to 100 (Tatterson, 1991). In this article we use $C = 100$. In general, we would like to keep the feed addition time as long as possible, that is,

$$t_f = t_p \tag{27a}$$

$$Ct_c \le n_f t_p \tag{27b}$$

Number of Feed Ports. From Eqs. 20a and 23a, it can easily be seen that the value of Da_m decreases with an increase in agitator speed (N) and power input per unit volume (P). However, because of economic reasons or equipment limitations, we cannot increase the power input per unit volume beyond a certain value ($P_{\max}$). The minimum value of Da_m, obtained at $P_{\max}$, is given by

$$Da_{m_{\min}} = \frac{12}{\ln 2} k_{\max} \left(\frac{\nu\rho}{P_{\max}} \right)^{1/2} \tag{28}$$

As noted in Step 1, we would like to operate in the perfectly mixed regime if possible and in the micromixing controlled regime otherwise. Thus, depending upon the minimum value of Da_m, we can place the following constraints on the values of the mixing index that we seek

$$\text{for } Da_{m_{\min}} > 0.01; \quad Q > Q_{\min} = 1.0 \tag{29a}$$

$$\text{for } Da_{m_{\min}} \le 0.01; \quad Q > Q_{\min} = Da_{m_{\min}}/0.01 \tag{29b}$$

Equation 29a ensures that we would operate in the micromixing controlled regime when operation in the perfectly mixed regime is infeasible. Equation 29b indicates that we are willing to operate at values of Q less than unity as long as we are in the perfectly mixed regime ($Da_s \le 0.01$). Using Eqs. 23c and 27a, we can write

$$t_p n_f \ge \frac{2^{7/6}}{\pi^{1/3}} \left(\frac{\ln 2}{12} \right)^3 Q_{\min}^3 \left(\frac{P_{\max}}{\rho N_p} \right)^{1/6} \frac{N_q^{1/2} \xi^{2/3} D^{8/3}}{a\nu^{3/2}} \tag{30}$$

where $Q_{\min}$ is given by Eq. 29a or 29b. As the number of feed ports has to be an integer, Eq. 30 leads to

$$n_f = \text{int}\left[\frac{2^{7/6}}{\pi^{1/3}} \left(\frac{\ln 2}{12} \right)^3 Q_{\min}^3 \left(\frac{P_{\max}}{\rho N_p} \right)^{1/6} \frac{N_q^{1/2} \xi^{2/3} D^{8/3}}{a t_p \nu^{3/2}} \right] + 1 \tag{31}$$

Table 4. Turbulent Power and Pumping Numbers for Agitator Types and Reactor Geometries Considered

Config.	N_p	N_q	References
A1	0.35	0.5	Oldshue (1983) Zlokarnik and Judat (1988)
A2	1.3	0.97	Bates et al. (1966) Fort (1986)
R1	5.0	0.75	Bates et al. (1966) Zlokarnik and Judat (1988) Tatterson (1991)
R2	4.0	0.95	Bates et al. (1966) Sano and Usui (1985) Tatterson (1991)
R3	2.6	0.85	Bates et al. (1966) Oldshue (1983) Tatterson (1991)
R4	0.75	0.29	Oldshue (1983) Zlokarnik and Judat (1988)

Table 5. Selection of Reactor Attributes and Operating Conditions for Example I

Config.	t_f (s)	n_f	$N_{\min}^{I}$ (rps)	$N_{\min}^{II}$ (rps)	$N_{\min}$ (rps)	$N_{\max}$ (rps)	$P_{\min}$ (W/m^3)	$P_{\max}$ (W/m^3)
A1	6,000	1	0.707	0.654	0.707	9.782	0.754	2,000
A2	6,000	1	0.364	0.423	0.423	6.317	0.599	2,000
R1	6,000	1	0.471	0.270	0.471	4.032	3.192	2,000
R2	6,000	1	0.372	0.290	0.372	4.343	1.257	2,000
R3	6,000	1	0.416	0.335	0.416	5.013	1.140	2,000
R4	6,000	1	0.361	0.261	0.361	3.895	1.593	2,000

$t_p = 6{,}000$ s; $P_{\max} = 2{,}000$ W/m^3; $Da_{m_{\min}} = 4.328$; $Q_{\min} = 1$; $Da_{m_{\max}} = 250$.

where the function int implies the highest integer lesser than the number within the square brackets.

For $n_f > 1$, the feed elements from each feed port should not interact with the feed elements from other feed ports (as this interaction has the same effect as self-engulfment). As there is no simple criterion to ensure this, it is advisable to keep the number of feed ports as small as possible. In some situations, it may be necessary to relax the production time constraint or the constraint on minimum value of Q to reduce the number of feed ports.

Agitator Speed. The upper bound on the agitator speed is given by the upper bound on P (Eq. 22)

$$N_{\max} = \left(\frac{\pi}{4} \frac{P_{\max}}{N_p \xi^5 D^2 \rho} \right)^{1/3} \tag{32}$$

Substituting Eq. 7 for t_c into Eq. 27, we get one lower bound on N given by

$$N_{\min}^{I} = \frac{\pi}{4} \frac{C}{N_q \xi^3 t_p n_f} \tag{33}$$

$N_{\min}^{I}$ gives the agitator rotational speed below which the circulation time is too long. As observed earlier, Da_m increases with decreasing agitator speed. We do not want Da_m to increase beyond a certain value ($Da_{m_{\max}}$). By combining Eqs. 22 and 23, this results in another lower bound on N given by

$$N_{\min}^{II} = \left(\frac{12}{\ln 2} \right)^{2/3} \left(\frac{\pi}{4} \right)^{1/3} \left(\frac{k_{\max}}{Da_{m_{\max}}} \right)^{2/3} \left(\frac{\nu}{N_p \xi^5 D^2} \right)^{1/3} \tag{34}$$

The lower bound on agitator speed is given by the higher of these two values

$$N_{\min} = \max\left(N_{\min}^{I}, N_{\min}^{II} \right) \tag{35}$$

Note that the reactor operation is not feasible if the lower bound thus obtained is higher than the upper bound, that is, if

$$N_{\min} > N_{\max} \tag{36}$$

In such a case, we have to relax the production time constraint or the constraint on the maximum value of Da_m to make the operation feasible.

Agitator Type and Reactor Geometry. Calculation of feed addition time, number of feed ports, and the range of agitator speeds for each configuration of agitator type and reactor geometry is implemented using a spreadsheet. The results of these calculations for Example I are presented in Table 5. Also shown are the ranges of power input per unit volume for these configurations corresponding to the ranges of operating speeds. The entire range of power inputs per unit volume can be divided into subranges based on the availability of configurations within these subranges. Equation 23a indicates that all configurations give the same Da_m for a given power input. Hence, within each subrange, we must choose the configuration that gives the highest value of Q from among those available. The subranges are shown in Figure 3. The bold lines show the values of Q that can be obtained by using the configuration of choice in each of these subranges. The configuration choices are indicated at the bottom of the

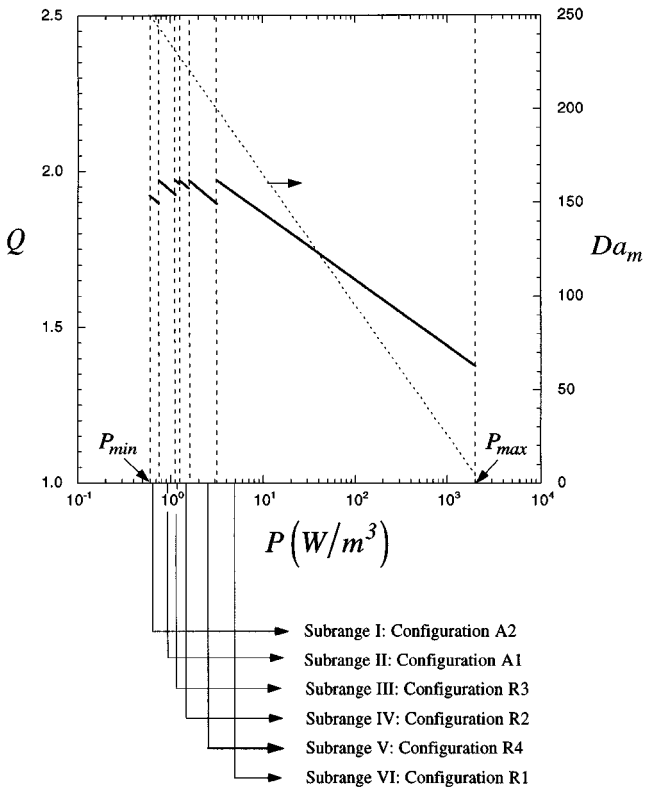

Figure 3. Reactor geometry and agitator type choices for Example I.

figure. Da_m as a function of power input per unit volume is shown by a dotted line.

In the entire operating range, Q is above unity and is not significantly affected by the power input. Da_m, on the other hand, decreases drastically as we go from $P_{\min}$ to $P_{\max}$. Thus, we have a tradeoff between operating cost and product distribution. For the best product distribution, we should operate at ($P = P_{\max}$) with configuration R1 (6-blade Rushton Turbine, $N = 4.032$ rps, $t_f = 6{,}000$ s, $n_f = 1$). If it is necessary to operate at lower power inputs for economic reasons, appropriate configuration should be selected from Figure 3.

Feed Location. The dependence of the local values of Da_m and Q on the local values of ϵ and u can be expressed (from Eqs. 3 and 6) as

$$Da_m \propto \epsilon^{-1/2} \tag{37a}$$

$$Q \propto u^{1/3}\epsilon^{-1/6} \tag{37b}$$

Local velocities are approximately related to the local rates of turbulent energy dissipation per unit mass as

$$u \propto \epsilon^{1/3} \tag{38}$$

Hence, in general, Da_m varies inversely with local values ϵ whereas Q stays relatively unaffected. Thus, for this example, we would like to choose the feed location that gives the highest value of ϵ and, therefore, the lowest value of Da_m. Highest values of ϵ are typically found in the plane of the agitator; especially in the agitator discharge. Hence, we would like the feed ports to be in the agitator plane, as close to the agitator as possible. If multiple feed ports are used, all ports should be located symmetrically at the same axial and radial positions for similar mixing environments.

Comments on Feedpipe Backmixing. Feedpipe backmixing is known to occur in agitated reactors and has experimentally been observed in laboratory reactors. The following empirical criterion is proposed by Fasano and Penney (1991) to prevent feedpipe backmixing

$$\begin{aligned} &u_f > 0.09\pi Nd; && \text{for feed location above the agitator} \\ &u_f > 0.5\pi Nd; && \text{for feed location in the agitator plane} \end{aligned} \tag{39}$$

where u_f is the feed velocity (m/s). The feed ports should be sized appropriately to satisfy Eq. 39.

Step 3: Selection of Heat-Transfer Policy. Heat transfer to or from the reacting mixture in an agitated reactor may be necessary for desired operation. In this step of the procedure, we select appropriate heat-transfer equipment for the reactor heat effects. The emphasis here is not on detailed design, but on selection of the best heat-transfer equipment for the given operation. Spatial inhomogeneity of temperature in agitated reactors is expected to be inconsequential. This is a good assumption for liquid-phase turbulent flow in agitated reactors as the thermal diffusivities of liquids are much higher than their mass diffusivities. It is for the same reason that we did not consider temperature effects in Steps 1 and 2.

To make the decision concerning the heat-transfer equipment, we first estimate the magnitude of the reactor heat load as follows

$$Q_G = |\Delta H|\frac{Q_f \rho}{M_f} + PV_R \tag{40}$$

where ΔH is the heat of reaction based on the conversion of the primary reactant (J/mol), and Q_f and M_f are the volumetric flow rate (m^3/s) and molecular weight, respectively, of the primary reactant. The magnitude of the heat-transfer capacity of the heat-transfer equipment may be expressed as

$$Q_R = UA_s|\Delta T| \tag{41}$$

where U is the overall heat-transfer coefficient ($W/m^2 \cdot K$), A_s is the total heat-transfer surface area (m^2), and $|\Delta T|$ is the magnitude of the temperature driving force. A simple criterion for suitability of a heat-transfer equipment type for the given operation is

$$Q_R \geq Q_G \tag{42}$$

Neglecting the resistance to heat transfer by the vessel or tube walls, we can express the overall heat-transfer coefficient as

$$U = \left(1/h_p + 1/h_f\right)^{-1} \tag{43}$$

where h_p is the heat-transfer coefficient on the process side ($W/m^2 \cdot K$) and h_f is the heat-transfer coefficient on the heat-transfer fluid side ($W/m^2 \cdot K$). h_p can be estimated using forced convection heat-transfer correlations of type

$$N_{Nu} = k_H N_{Re}^{2/3} N_{Pr}^{1/3} \tag{44}$$

where

$$N_{Nu} = h_p D/\lambda \tag{45a}$$

and

$$N_{Pr} = \mu C_p/\lambda \tag{45b}$$

In Eq. 44, we have neglected the viscosity correction factor. Values between 0.3 and 1.2 have been reported for the constant k_H in the literature (Uhl, 1966; Nagata, 1975; Bolliger, 1986; Bondy and Lippa, 1986; Oldshue, 1983; Shah, 1991). Here, as suggested by Shah (1991), we use $k_H = 0.5$ for axial flow agitators (configurations A1 and A2) and $k_H = 0.8$ for radial flow agitators (configurations R1 to R4). More detailed correlations for k_H for various combinations of agitator types and reactor geometry can be obtained from the above references. Using Eq. 43, the criterion of Eq. 42 can thus be rewritten as

$$\frac{1}{h_f}\frac{A_s^{\text{ref}}}{A_s} \leq \frac{|\Delta T|\, A_s^{\text{ref}}}{Q_G} - \frac{1}{h_p}\frac{A_s^{\text{ref}}}{A_s} \tag{46}$$

Table 6. Heat-Transfer Equipment Considered

(1) *External Heat-Transfer Jackets*
(a) Simple jacket (tank-in-tank type)
(b) Jacket with agitation nozzles
(c) Jacket with spiral baffles
(d) Dimpled jacket
(e) Partial pipe type jacket
(2) *Internal Coils*
(a) Helical coils
(b) Coils meandering along the wall
(c) Coil bundles as baffles

Here, A_s^{ref} $(=\pi D^2)$, which is the area of the cylindrical surface of the reactor, serves as a reference. Note that in the above equation, as h_p is evaluated using Eq. 44, h_f and A_s are the only parameters which depend on the equipment used for heat transfer. The most common heat-transfer equipment used industrially is listed in Table 6. The literature information about h_f and A_s (Uhl, 1966; Nagata, 1975; Bolliger, 1986; Bondy and Lippa, 1986) for these equipment units can be summarized in the form of generic parameter maps. Figure 4a shows the parameter map for the heat-transfer surface area. The heat-transfer area A_s is normalized with A_s^{ref} to eliminate its dependence on reactor size. From this parameter map, we can see that for all heat exchanger types, the ratio A_s/A_s^{ref} lies close to unity. Hence, using $A_s/A_s^{\text{ref}}=1$ in the second term on the righthand side of Eq. 46 and rearranging, we get

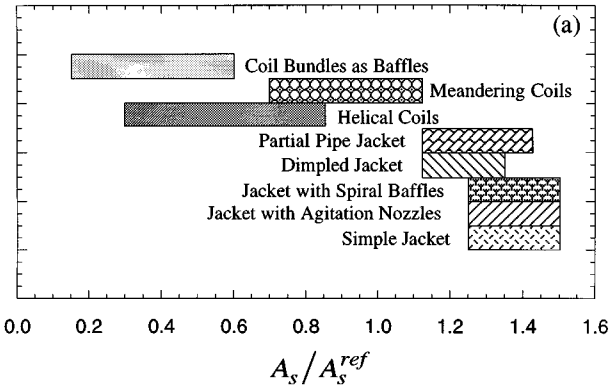

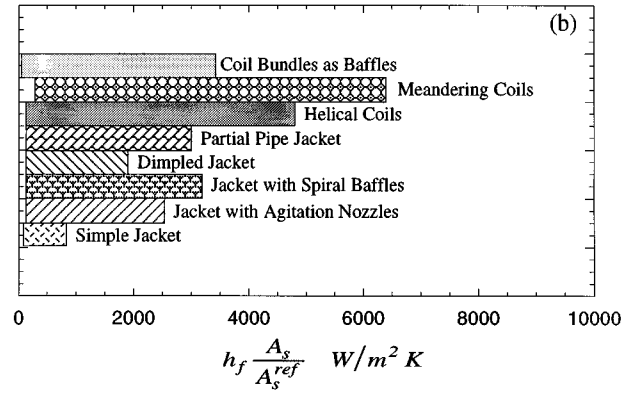

Figure 4. Generic parameter maps for heat-transfer equipment under consideration.

(a) A_s/A_s^{ref}; (b) $h_f(A_s/A_s^{\text{ref}})$.

$$h_f\frac{A_s}{A_s^{\text{ref}}} \geq \frac{h_p Q_G}{\left(|\Delta T|\, A_s^{\text{ref}} h_p - Q_G\right)} \tag{47}$$

Now, the parameter on the righthand side of this criterion is a function only of reactor attributes and operating conditions which have already been decided. Thus, its value can easily be calculated. The parameter on the lefthand side is a function of the heat-transfer equipment and the properties of the heat-transfer fluid. A generic parameter map for this parameter is given in Figure 4b. Based on the value of the parameter on the righthand side and the parameter map of Figure 4b, it is a simple matter to see for which heat-transfer equipment Eq. 47 is satisfied. All equipment types that satisfy Eq. 47 can be used satisfactorily. Frequently, there will be more than one equipment type available for the desired operation. In such cases, the following heuristics can be used to choose one of them.

- Use the simplest and most economical type of jacket or internal coil configuration whenever possible. Different types of external jackets and internal coils are arranged in approximate order of increasing cost in Table 6.
- Do not use internal coils for pharmaceutical applications.
- Do not use jacket types 1a, 1b, and 1c when pressure on the heat-transfer fluid side exceeds 150 psi; jacket type 1d when pressure exceeds 300 psi; and jacket type 1e when pressure exceeds 750 psi.

It should be noted that for Eq. 47 to be valid, the process side heat-transfer coefficient should be sufficiently high, that is,

$$h_p \geq \frac{Q_G}{|\Delta T|\, A_s^{\text{ref}}} \tag{48}$$

If the criteria of Eq. 47 or Eq. 48 are not satisfied for any of the above equipment, additional heat-transfer methods such as addition of a heat carrier may be considered or some of the process constraints (such as the production time constraint) may be relaxed. In such cases, Steps 1 and 2 have to be repeated as any such measures would influence the decisions made in these steps.

Step 3 for Example I. Based on the information of Table 2 and the reactor attributes and operating conditions chosen in the previous step, we have

$$Q_G = 5.093\times 10^4 \text{ W} \tag{49a}$$

$$h_p = 4.4385\times 10^3 \text{ W/m}^2\cdot\text{K} \tag{49b}$$

and

$$h_f\frac{A_s}{A_s^{\text{ref}}} \geq \frac{h_p Q_G}{\left(|\Delta T|\, A_s^{\text{ref}} h_p - Q_G\right)} = 2.0235\times 10^3 \text{ W/m}^2\cdot\text{K} \tag{49c}$$

For a temperature driving force of 10 K, the process side heat-transfer coefficient is sufficiently high to satisfy Eq. 48. Also from Eq. 49c and Figure 4b, the heat-transfer requirements can be satisfactorily met by using equipment types 1b, 1c, 1e, 2a, 2b, or 2c. Of these, the jacket with agitation nozzles (1b) is the most economical and should be used. Let us now consider two additional examples to illustrate the procedure.

Example II: parallel reactions

Consider a five component system with two reactions in parallel

$$\begin{aligned} A + B &\rightarrow D \\ B + C &\rightarrow E \end{aligned} \tag{50}$$

Here, C is the product of interest and A is a byproduct or unconverted reactant carried over from previous processing steps. Before further processing, it is necessary to convert A to D by addition of B. However, this also leads to the undesired reaction involving the loss of product C. Thus, the objective is to minimize the product distribution which is expressed as

$$\text{Product Distribution} = \frac{E \text{ Produced}}{B \text{ Reacted}} \tag{51}$$

Other input information is summarized in Table 7. Such situations are frequently encountered in the pharmaceutical industry, such as pH adjustment by acid/base addition in presence of labile substrates (Paul et al., 1992). Here, let us consider the synthesis of a laboratory-scale reactor ($D = 0.5$ m).

Step 1: Estimation of Reactor Performance and Choice of Operating Regime. Figures 5a and 5b depict the reactor performance in various operating regimes. As expected, for a given Da_m, the product distribution is lower in the micromixing controlled regime and increases as we move towards the mesomixing controlled regime. Also, for a given Q, the product distribution becomes more favorable with decreasing Da_m. Therefore, we would like to operate in the perfectly mixed regime ($Q > 1$, $Da_m \ll 1$ or $Q < 1$, $Da_s \ll 1$) if feasible, or in the micromixing controlled regime with the minimum value of Da_m otherwise.

Table 7. Input Information for Example II

Information about the reactions
$A + B \rightarrow D$; $\quad R_1 = k_1 x_A x_B$
$B + C \rightarrow E$; $\quad R_2 = k_2 x_B x_C$
$k_1 = 6.174 \times 10^6 \exp[-4{,}000/T(\text{K})]\ \text{s}^{-1}$
$k_2 = 6.174 \times 10^5 \exp[-4{,}000/T(\text{K})]\ \text{s}^{-1}$
$k_1 = 10\,k_2 = 10\ \text{s}^{-1}$ @ $T = 300$ K
$\Delta H = -2.3 \times 10^4$ J/mol·B reacted
Information about the components
Pure B and equimolar mixture of A and C are used as reactants.
$\rho = 1.2 \times 10^3$ kg/m^3 — $M_A = 1{,}000$ g/mol
$\nu = 2 \times 10^{-6}$ m^2/s — $M_B = 120$ g/mol
$C_p = 4.18 \times 10^3$ J/kg·K — $M_C = 2{,}000$ g/mol
$\lambda = 0.9$ W/m·K — $M_D = 1{,}120$ g/mol
$M_E = 2{,}120$ g/mol
Information about the process
Semibatch addition of B
Isothermal operation at 300 K
Reactor size = 98.2 L ($D = 0.5$ m)
Max. production time for the reactor (t_p) = 360 s
Max. power input/unit vol. ($P_{\max}$) = 2,000 W/m^3

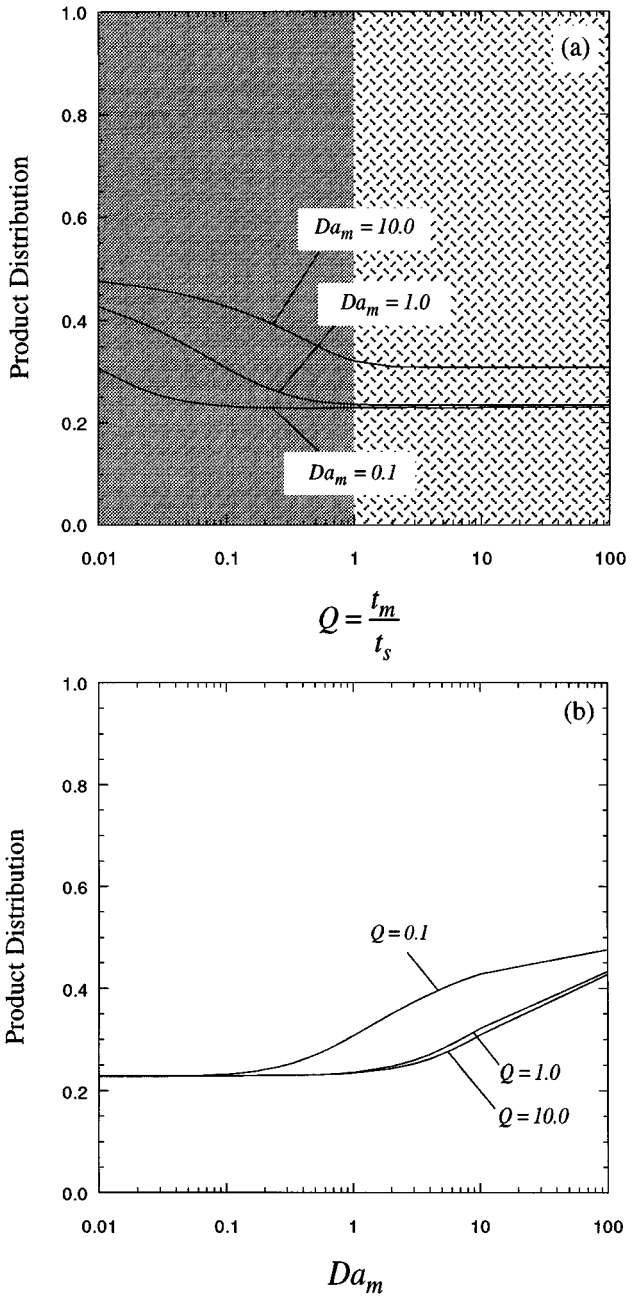

Figure 5. Reactor performance in various operating regimes for Example II.

(a) Product distribution as a function of mixing index; (b) product distribution as a function of Damköhler number for micromixing.

Step 2: Selection of Reactor Attributes and Operating Conditions. The details of this step are summarized in Table 8. As Da_m cannot be decreased below 0.1896, we have to ensure that the reactor is operated in the micromixing controlled regime ($Q > Q_{\min} = 1$). Results indicate that the use of con-

Table 8. Selection of Reactor Attributes and Operating Conditions for Example II

Config.	t_f (s)	n_f	$N_{\min}^{I}$ (rps)	$N_{\min}^{II}$ (rps)	$N_{\min}$ (rps)	$N_{\max}$ (rps)	$P_{\min}$ (W/m^3)	$P_{\max}$ (W/m^3)
A1	360	2	5.888	5.075	5.888	15.382	112.255	2,000
A2	360	2	3.035	3.277	3.277	9.933	71.902	2,000
R1	360	1	7.850	2.092	7.850	6.339	3,801.214	2,000
R2	360	1	6.197	2.253	6.197	6.829	1,496.323	2,000
R3	360	1	6.926	2.601	6.926	7.883	1,357.853	2,000
R4	360	1	6.015	2.021	6.015	6.125	1,896.269	2,000

$t_p = 360$ s; $P_{\max} = 2{,}000$ W/m^3; $Da_{m_{\min}} = 0.1896$; $Q_{\min} = 1$; $Da_{m_{\max}} = 1$.

figuration R1 is not advisable (Eq. 36). Other configurations can be used, however, and the ranges of operating speeds and power inputs over which their operation is feasible are shown in Table 8. The entire range of power inputs is divided into subranges depending on the availability of configurations within each subrange (Figure 6). As before, in each subrange, we choose the configuration that gives the highest value for Q. The bold lines show the values of Q in each subrange obtained by using the selected configuration and the dotted line shows the values of Da_m. Similar to the previous example, a trade-off between power input per unit volume and Da_m is observed. For best results, we use configuration A1 (three-blade marine propeller) with $N = 9.933$ rps, $t_f = 360$ s, and $n_f = 2$.

Note that two feed ports are required for configurations A1 and A2, while only one feed port is required for R2, R3, and R4. Configurations R2, R3, or R4 can also be used with two feed ports, in which case the subranges and the configuration choices in these subranges would be different. Configurations A1 and A2 should not be considered if we do not want to have more than one feed port.

Step 3. Selection of Heat-Transfer Policy. Here we have

$$Q_G = 5.1372 \times 10^3 \text{ W} \tag{52a}$$

$$h_p = 7.5251 \times 10^3 \text{ W/m}^2\cdot\text{K} \tag{52b}$$

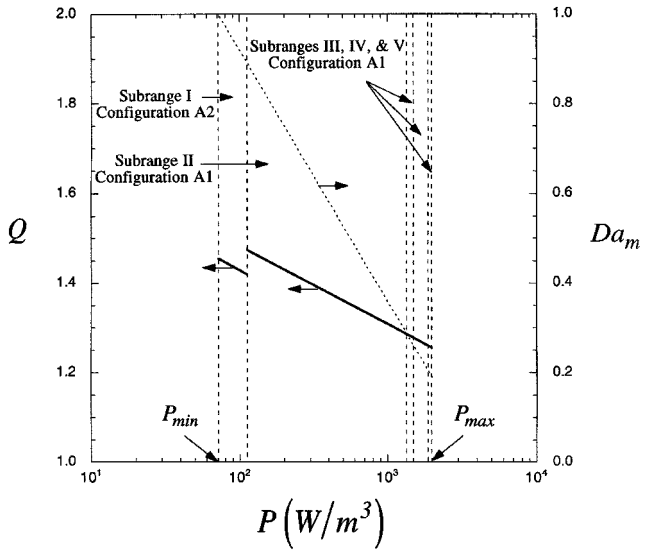

Figure 6. Reactor geometry and agitator type choices for Example II.

and hence

$$h_f \frac{A_s}{A_s^{\text{ref}}} \geq 0.7164 \times 10^3 \text{ W/m}^2\cdot\text{K} \tag{52c}$$

All equipment types can thus be used satisfactorily, the simplest being the common tank-in-tank type jacket (type 1a).

Example III: complex consecutive-competing reactions

Let us consider a five component system with a complex network of three consecutive-competing reactions:

$$\begin{aligned} A + B &\rightarrow C \\ B + C &\rightarrow D \\ B + D &\rightarrow E \end{aligned} \tag{53}$$

Here, the desired product D is produced by the first set of consecutive-competing reactions. D, however, is also involved in the second set of consecutive-competing reactions which produce the undesired product E. One way of defining the product distribution in this case is

$$\text{Product Distribution} = \frac{D \text{ Produced}}{E \text{ Produced}} \tag{54}$$

The objective is to maximize the product distribution as defined above. This example represents a reaction system discussed by Paul (1988). Relevant input information is presented in Table 9.

Step 1: Estimation of Reactor Performance and Choice of Operating Regime. Reactor performance in various operating regimes is shown in Figures 7a and 7b. As clearly evident from these figures, we would like to operate in the perfectly mixed regime ($Q > 1$, $Da_m \ll 1$ or $Q < 1$, $Da_s \ll 1$) if feasible, or in the micromixing controlled regime with the minimum value of Da_m otherwise.

Step 2: Selection of Reactor Attributes and Operating Conditions. Table 10 presents the summary of calculations done at this step. As the reactions are much slower than the previous examples ($Da_{m_{\min}} = 0.0061 < 0.01$), operation in the perfectly mixed regime is feasible. Hence, we are willing to operate at values of Q lesser than unity ($Q_{\min} = 0.61$). The range of power inputs per unit volume is identical for all configurations. Over this range, configuration A2 (6-blade pitched blade turbine, $N = 3.61$ rps, $t_f = 18{,}000$ s, $n_f = 2$) gives the highest value of Q and should be used. Figure 8 shows the values of Q (bold line) and Da_m (dotted line) as a function of power input per unit volume.

Table 9. Input Information for Example III

Information about the reactions	
$A + B \rightarrow C;$	$R_1 = k_1 x_A x_B$
$B + C \rightarrow D;$	$R_2 = k_2 x_B x_C$
$B + D \rightarrow E;$	$R_3 = k_3 x_B x_D$
$k_1 = 1.213 \times 10^8 \exp[-6{,}000/T(\mathrm{K})]\ \mathrm{s}^{-1}$	
$k_2 = 1.213 \times 10^8 \exp[-6{,}000/T(\mathrm{K})]\ \mathrm{s}^{-1}$	
$k_3 = 2.426 \times 10^8 \exp[-6{,}000/T(\mathrm{K})]\ \mathrm{s}^{-1}$	
$k_3 = 2k_1 = 2k_2 = 0.5\ \mathrm{s}^{-1}$ @ $T = 300$ K	
$\Delta H = -5.75 \times 10^5$ J/mol·B reacted	
Information about the components	
Pure A and B are used as reactants.	
$\rho = 10^3$ kg/m^3	$M_A = 1{,}000$ g/mol
$\nu = 1 \times 10^{-6}$ m^2/s	$M_B = 60$ g/mol
$C_p = 4.18 \times 10^3$ J/kg·K	$M_C = 1{,}060$ g/mol
$\lambda = 0.614$ W/m·K	$M_D = 1{,}120$ g/mol
	$M_E = 1{,}180$ g/mol
Information about the process	
Semibatch addition of B	
Isothermal operation at 300 K	
Reactor size = 12,272 L ($D = 2.5$ m)	
Max. production time for the reactor (t_p) = 18,000 s	
Max. power input/unit vol. ($P_{\max}$) = 2,000 W/m^3	

Note that the trade-off between P and Da_m is not important here as we operate in the perfectly mixed regime for all values of P. Thus, it is not necessary to operate the agitator at $N = N_{\max}$. Also, as long as $Q > Q_{\min}$, the value of Q does not influence the performance. Hence, any other configuration can be equivalently used in place of configuration A2.

Step 3. Selection of Heat-Transfer Policy. Based on the input information and the decisions made above

$$Q_G = 3.267 \times 10^5 \text{ W} \tag{55a}$$

$$h_p = 4.2950 \times 10^3 \text{ W/m}^2\cdot\text{K} \tag{55b}$$

and hence,

$$h_f \frac{A_s}{A_s^{\text{ref}}} \geq 2.7155 \times 10^3 \text{ W/m}^2\cdot\text{K} \tag{55c}$$

Equipment types 1c, 1e, 2a, 2b and 2c can thus be used satisfactorily.

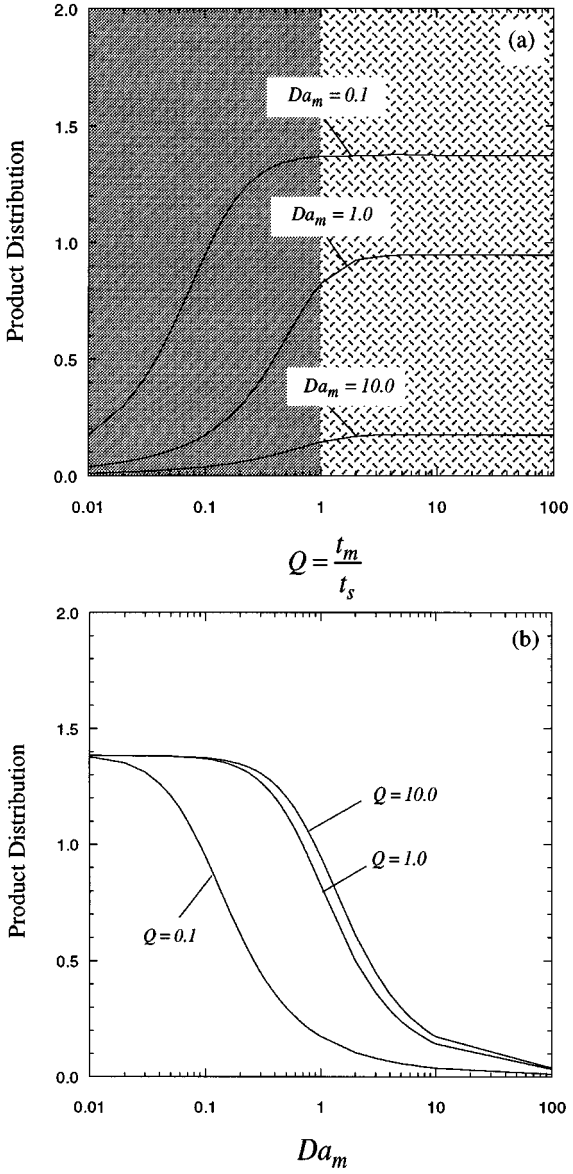

Figure 7. Reactor performance in various operating regimes for Example III.

(a) Product distribution as a function of mixing index; (b) product distribution as a function of Damköhler number for micromixing.

Simulation of Single-Phase Agitated Reactors

As discussed, average flow properties (u_{avg} and ϵ_{avg}) were used to evaluate the mixing time scales (t_m and t_s) and the governing dimensionless numbers (Da_m and Q) in the synthesis component. This enabled us to reliably choose from a large number of combinations of reactor attributes and operating conditions without excessive time and effort. After choosing the reactor attributes and operating conditions, it may be necessary to evaluate the performance of the chosen reactor by accounting for the spatial variations in flow properties. In some cases, such performance evaluation (for laboratory-scale reactors) may be used in conjunction with experiments to gain more insights into the process.

The principles of simulation are presented by Baldyga and Bourne (1988). The flow field is assumed to be steady and the spatial distributions of time-averaged flow velocity (u) and the rate of energy dissipation (ϵ) are obtained from experiments, CFD, or a combination of both. It is also assumed that the incoming fluid elements retain their identities and their history can be tracked (that is, their current position can be determined from the knowledge of the feed location and their age).

Use of experimental flow models

A large body of information exists on experimental studies on flow in agitated reactors of different geometries and agitator types (Nagata, 1975; Ranade and Joshi, 1989, 1990a; Wu and Patterson, 1989; Tatterson, 1991; Schafer et al., 1998;

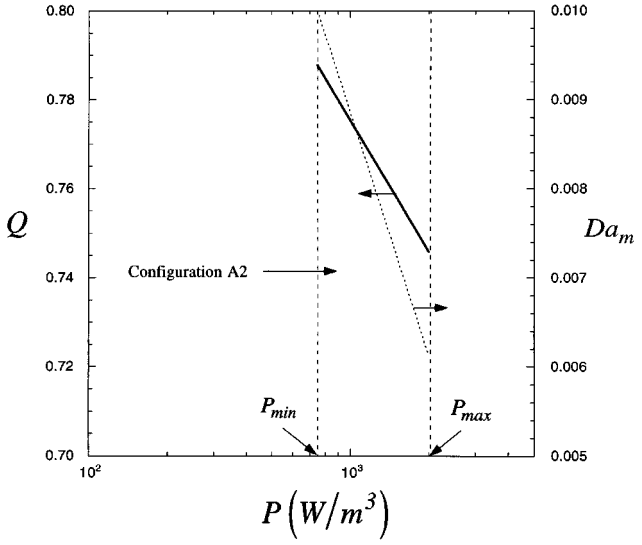

Figure 8. Reactor geometry and agitator type choices for Example III.

among others). Configuration R1 (6-blade Rushton turbine) is the most widely studied configuration. On the basis of 61 experimental studies involving this configuration, Bourne and Yu (1994) have constructed a simplified model that describes spatial variations of u and ϵ. This model is called the Experimental Flow Model (EFM) and is shown in Figure 9.

Let us demonstrate the use of the EFM by evaluating the performance of reactor configuration R1 for the reaction system of Example II with $D = 0.5$ m, $N = 2.3355$ rps, $t_f = 1{,}800$ s, $n_f = 1$, and heat transfer through an external jacket. Figure 10a shows the reactor performance for feed locations at different radial and axial positions. The product distribution varies for each feed location as the incoming fluid elements spend different amounts of time in regions of different values of ϵ. As expected, for all radial locations, the most favorable product distribution is obtained in the agitator plane. Here, the fluid elements are convected away from the agitator. The closer the feed addition to the agitator, the longer is the time the fluid elements spend in the region of high ϵ. Hence, the product distribution becomes more favorable as r decreases. Also, for all radial locations, the product distribution becomes increasingly less favorable as we move away from the agitator plane. For the operating conditions chosen for this example, the product distribution is not very sensitive to the feed location. Figure 10b shows the effects of feed addition

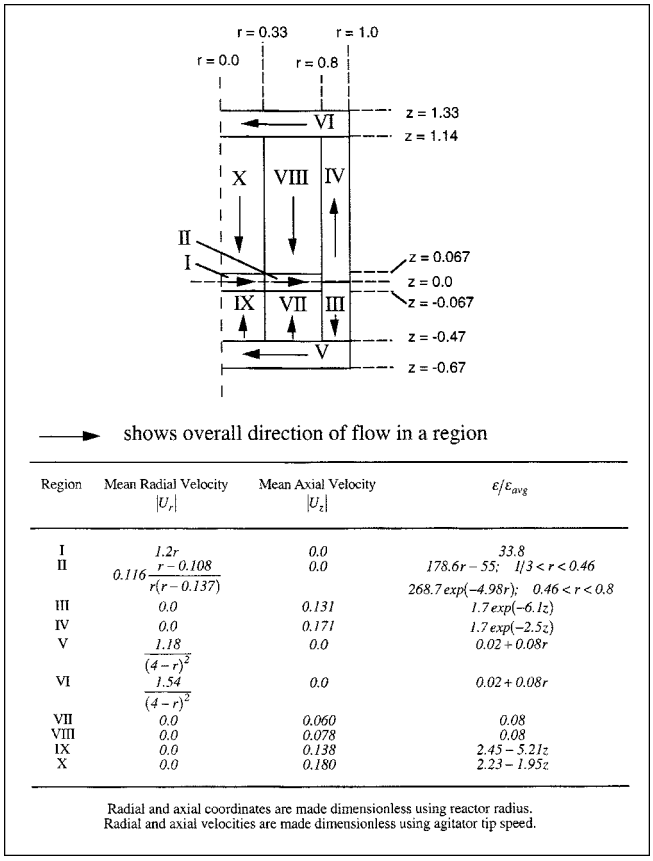

Region	Mean Radial Velocity $\lvert U_r \rvert$	Mean Axial Velocity $\lvert U_z \rvert$	ϵ/ϵ_{avg}
I	$1.2r$	0.0	33.8
II	$0.116\dfrac{r-0.108}{r(r-0.137)}$	0.0	$178.6r-55$; $1/3<r<0.46$ $268.7\exp(-4.98r)$; $0.46<r<0.8$
III	0.0	0.131	$1.7\exp(-6.1z)$
IV	0.0	0.171	$1.7\exp(-2.5z)$
V	$\dfrac{1.18}{(4-r)^2}$	0.0	$0.02+0.08r$
VI	$\dfrac{1.54}{(4-r)^2}$	0.0	$0.02+0.08r$
VII	0.0	0.060	0.08
VIII	0.0	0.078	0.08
IX	0.0	0.138	$2.45-5.21z$
X	0.0	0.180	$2.23-1.95z$

Radial and axial coordinates are made dimensionless using reactor radius.
Radial and axial velocities are made dimensionless using agitator tip speed.

Figure 9. Experimental flow model for configuration R1.
Based on Bourne and Yu (1994).

time on the product distribution. For $t_f = t_p = 1{,}800$ s, the average value of the mixing index is 2.18. Hence, we are barely into the micromixing controlled regime and, as the feed addition time decreases, we move towards the mesomixing controlled regime, thus making the product distribution less favorable. Figure 10c shows the the product distribution becomes less favorable with decreasing agitator speed. As the agitator speed decreases, the average values of both Q and Da_m increase (Eqs. 20a and 20c). The increase in Da_m ($\sim N^{-3/2}$) is however much more significant than the increase in Q ($\sim N^{-1/6}$) and, therefore, the product distribution becomes less favorable. The above observations confirm the decisions we made in the synthesis procedure about feed location, agitator speed, and feed addition time.

Table 10. Selection of Reactor Attributes and Operating Conditions for Example III

Config.	t_f (s)	n_f	$N^{\mathrm{I}}_{\min}$ (rps)	$N^{\mathrm{II}}_{\min}$ (rps)	$N_{\min}$ (rps)	$N_{\max}$ (rps)	$P_{\min}$ (W/m^3)	$P_{\max}$ (W/m^3)
A1	18,000	1	0.236	4.028	4.028	5.590	748.977	2,000
A2	18,000	2	0.061	2.601	2.601	3.610	748.977	2,000
R1	18,000	1	0.157	1.660	1.660	2.304	748.977	2,000
R2	18,000	1	0.124	1.788	1.788	2.482	748.977	2,000
R3	18,000	1	0.139	2.064	2.064	2.865	748.977	2,000
R4	18,000	1	0.120	1.604	1.604	2.226	748.977	2,000

$t_p = 18{,}000$ s; $P_{\max} = 2{,}000$ W/m^3; $Da_{m_{\min}} = 0.0061$; $Q_{\min} = 0.61$; $Da_{m_{\max}} = 0.01$.

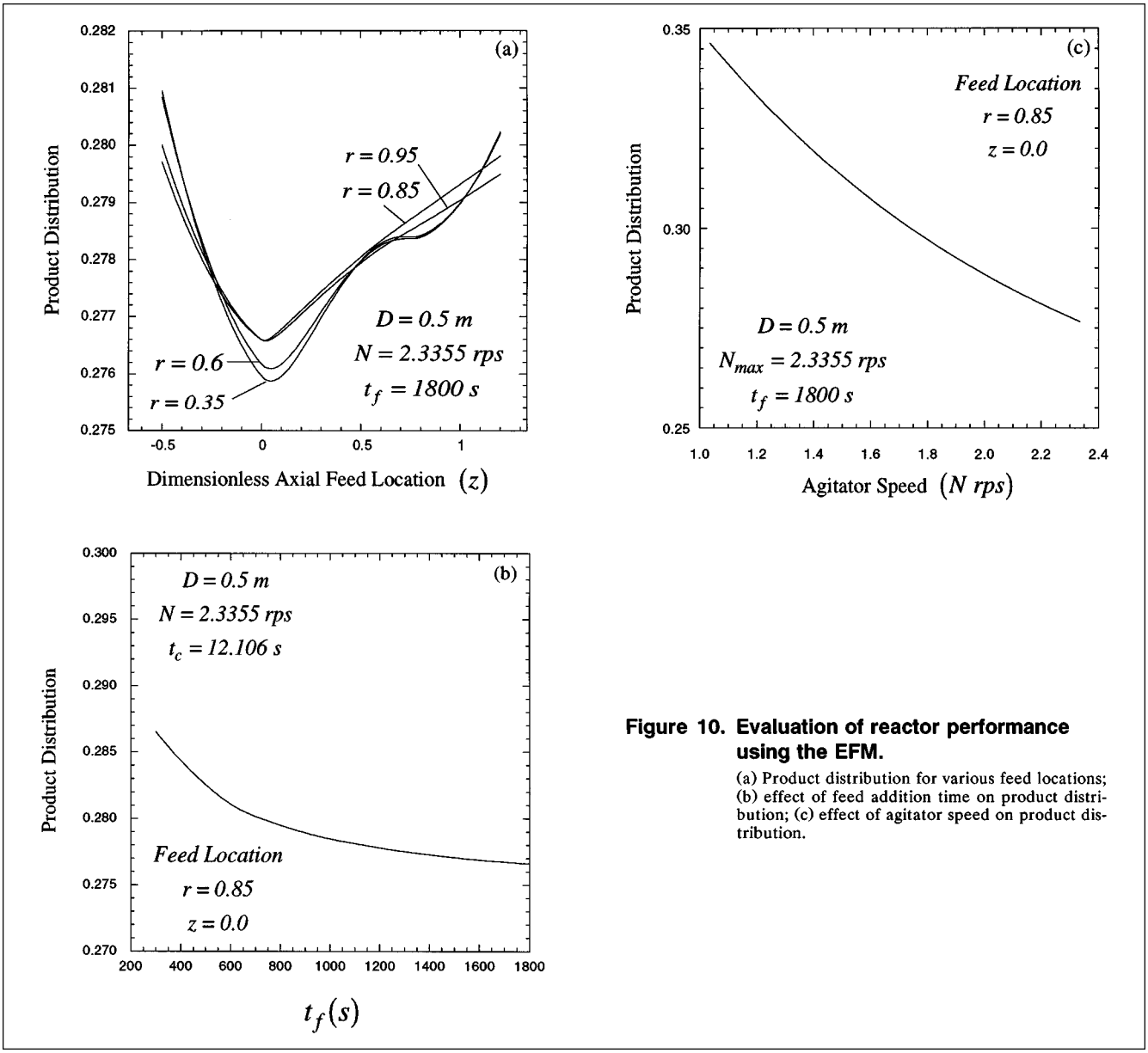

Figure 10. Evaluation of reactor performance using the EFM.

(a) Product distribution for various feed locations; (b) effect of feed addition time on product distribution; (c) effect of agitator speed on product distribution.

Use of CFD simulations

Experimental flow models represent the characteristics of the flow in agitated reactors, but certainly oversimplify the complexity of actual flow. CFD simulations (agitator boundary conditions being supplied by experimental measurements) offer another option to predict the flow properties for different geometrical and operating conditions (Ranade, 1995). In recent years, CFD applications have received a lot of attention and a number of CFD studies on flow in different reactor configurations have been reported (Ranade et al., 1989; Ranade and Joshi, 1990b; Kresta and Wood, 1991; among others).

Here, let us consider the parallel reaction system of Example II in a conventional laboratory-scale reaction calorimeter. For the given reactor geometry, agitator type, and agitator speed, the velocity field and the rates of turbulent energy dissipation are obtained from CFD simulations using the k-ϵ model. The effect of feed addition time on product distribution for feed addition at different locations is studied as before and the results are presented in Figure 11. At any feed location, mesomixing becomes increasingly significant as the feed addition time decreases. Hence, the product distribution increases (becomes less favorable) with faster feed addition. Also, for a given feed addition time, the product distribution is expectedly more favorable in the agitator plane and becomes less favorable as we move away from the agitator.

Scaleup of Single-Phase Agitated Reactors

Often, agitated reactors are scaled up from the laboratory scale to the production scale due to the need of quick time-to-market. The production-scale reactor is geometrically similar to the lab-scale reactor and the same mode of operation

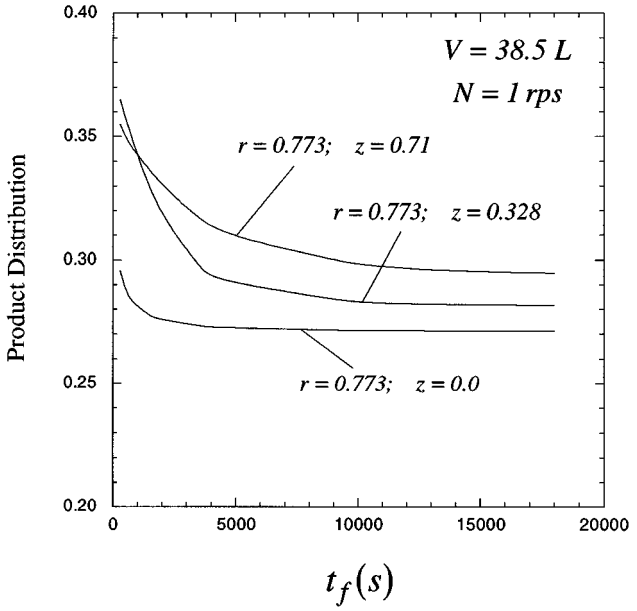

Figure 11. Evaluation of reactor performance using CFD: effect of feed addition time on product distribution for various feed locations.

Radial and axial coordinates are made dimensionless by using reactor radius.

is followed. The objective is to at least preserve the reactor performance that was obtained at the laboratory scale by following some scale-up rules. In this section, we will develop scaleup rules based on the interplay of reaction and various mixing scales discussed previously using average flow properties.

As seen from the three examples considered, in most situations, we would like to operate in the perfectly mixed regime if possible or in the micromixing controlled regime with a low value of Da_m. The objective function deteriorates as we move into the meso- and macromixing controlled regimes. Thus, to improve or at best preserve the product distribution, the scale-up rules should meet the following three requirements with increasing reactor size: (1) Da_m should decrease or remain constant; (2) Q should increase or remain constant; and (3) $t_f n_f/t_c$ should increase or remain constant.

From Eqs. 23a, 23c and 24, as all other variables are constant for all reactor sizes, we get

$$Da_m \propto P^{-1/2} \tag{56a}$$

$$Q \propto t_f^{1/3} D^{-8/9} P^{-1/18} \tag{56b}$$

$$t_f n_f/t_c \propto t_f D^{-2/3} P^{1/3} \tag{56c}$$

Table 11. Scale-Up Rules for Agitated Reactors

Rule	β	δ	Desired δ (Eq. 58b)
Constant Power/ Unit Vol.	0	0	8/9
Constant Agitator Tip Speed	$-1/3$	0	—
Constant Circulation Time	2/3	0	1

Clearly, the power input per unit volume P and the feed addition time (or equivalently, the average residence time for continuous operation) t_f are the only variables that can be manipulated. Let these manipulated variables change with reactor volume as

$$P \propto V^{\beta} \tag{57a}$$

$$t_f \propto V^{\delta} \tag{57b}$$

Substituting into Eqs. 56a to 56c, we obtain the following conditions to satisfy the above three requirements

$$\beta \geq 0 \qquad \text{for requirement 1} \tag{58a}$$

$$\delta \geq \frac{\beta}{6} + \frac{8}{9} \qquad \text{for requirement 2} \tag{58b}$$

$$\delta \geq -\frac{\beta}{3} + \frac{2}{9} \qquad \text{for requirement 3} \tag{58c}$$

Note that for $\beta \geq 0$, Eq. 58c is always satisfied when Eq. 58b is satisfied. Hence, we will ignore Eq. 58c. Equations 57a and 57b give the ideal scale-up rule with the indices being constrained by Eqs. 58a and 58b.

Several scale-up rules have been proposed and experimentally studied in the literature such as: constant power input per unit volume (Bourne and Dell'Ava, 1987; Bourne and Yu, 1994); constant agitator tip speed (Paul and Treybal, 1971); and constant circulation time (Fasano and Penney, 1991; Tipnis et al., 1994). As is obvious from the equations above, the feed addition time should also be considered as a manipulated variable. However, in most of the studies, the feed addition time is kept constant. Only a few authors (Fasano and Penney, 1991; Bourne and Yu, 1994) consider the effect of changes in feed addition time, although it is not explicitly included in the proposed scale-up rule. The values of β and δ for these scale-up rules are summarized in Table 11. Clearly, constant agitator tip speed criterion is not a good scale-up rule as $\beta < 0$. For the other two rules, $\beta \geq 0$. However, the constraint given by Eq. 58b is not satisfied. The desired values of δ for these rules are also given in Table 11 for the sake of comparison.

In view of the literature studies and the discussion above, let us analyze the range of applicability of the following scale-up rules:

- *Rule 1:* constant P, constant t_f ($\beta = 0$; $\delta = 0$).
- *Rule 2:* constant P, $t_f \propto D^{8/3}$ ($\beta = 0$; $\delta = 8/9$).
- *Rule 3:* constant t_c, constant t_f ($\beta = 2/3$; $\delta = 0$).
- *Rule 4:* constant t_c, $t_f \propto D^3$ ($\beta = 2/3$; $\delta = 1$).

Rule 4 clearly is the most suited as it will decrease Da_m and increase Q and $t_f n_f/t_c$ with reactor size, thus improving the performance. However, it calls for higher power input per unit volume and longer feed addition times with increasing reactor size. Similarly, Rule 3 calls for an increase in P with reactor size, and Rule 2 calls for higher t_f as the reactor size increases. In many situations, it may not be possible to increase P and t_f due to the operating constraints ($P_{\max}$ and t_p). In view of these constraints, Rule 1 is the most suited as it does not require any increase in P and t_f. However, it may not improve or preserve the performance as the requirements of Eq. 58b are not satisfied. Therefore, before using

any of the above rules, the trade-off between performance and operating constraints must be carefully considered. The following general conclusions can be drawn:

(1) Use Rule 4, if both P and t_f can be increased without bound.

(2) Use Rule 3, if t_f cannot be increased and P can be increased without bound.

(3) Use Rule 2, if P cannot be increased and t_f can be increased without bound.

(4) Use Rule 1, if both P and t_f cannot be increased.

(5) Use Rule 1 (if t_f cannot be increased) or Rule 2 (if t_f can be increased) if operation in the perfectly mixed regime or the micromixing controlled regime is feasible at the largest reactor size, that is, if the following conditions are satisfied at the largest reactor size

$$\begin{aligned} Q &> 1; && \text{for } Da_m > 0.01 \\ Q &> Da_m/0.01; && \text{for } Da_m \le 0.01 \end{aligned} \tag{59a}$$

$$t_f n_f / t_c \ge 100 \tag{59b}$$

The last conclusion is based on the fact that, in the perfectly mixed regime or in the micromixing controlled regime, the reactor performance is insensitive to the value of the mixing index. Therefore, we do not want to spend on additional power input per unit volume, as this may not lead to significant improvement in performance.

Let us now demonstrate these rules. We begin with the reaction system of Example III. Here, the reactions are relatively slow and, hence, the operation in the perfectly mixed regime is feasible. Let us consider a laboratory-scale reactor ($D = 0.2$ m) of configuration R4 with $N = 9.516$ rps, $n_f = 1$, and $t_f = 3{,}600$ s. Figure 12 shows a comparison of Rules 1 and 3. The product distribution obtained is the same for both rules and also the same for all reactor sizes. This is because we operate in the perfectly mixed regime for all reactor sizes

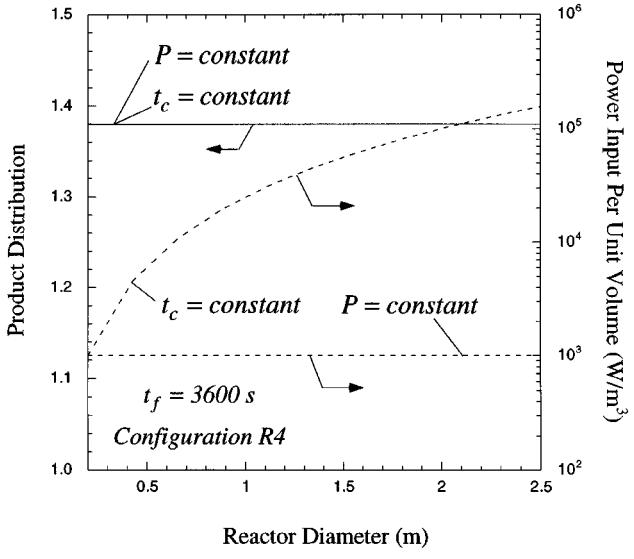

Figure 12. Comparison of scale-up Rules 1 and 3 for Example III.

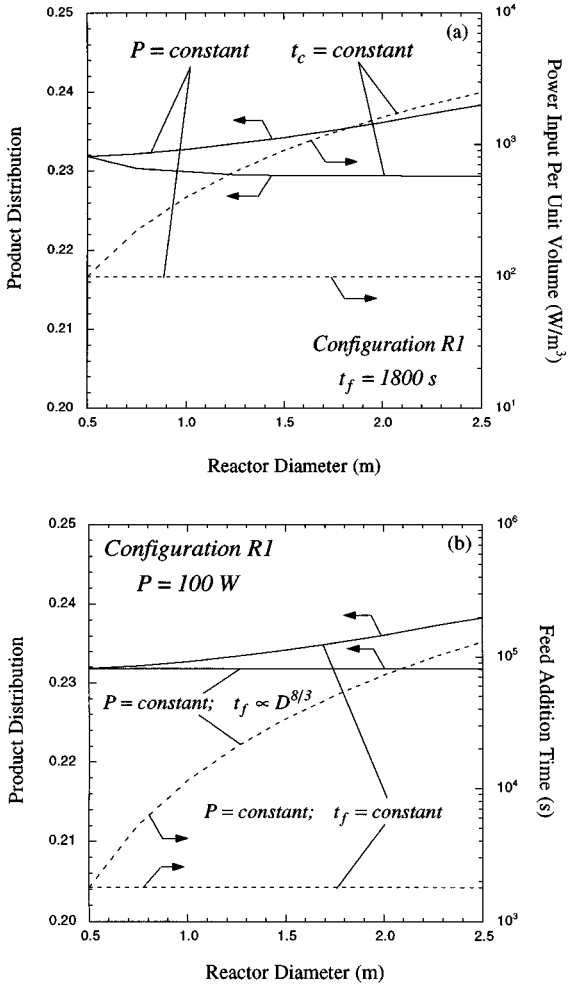

Figure 13. Comparison of scale-up rules for Example II.

(a) Rules 1 and 3; (b) Rules 1 and 2.

and decrease in the value of the mixing index with reactor size does not affect the product distribution. Power input per unit volume corresponding to both the rules is also shown in Figure 12 by dashed lines. While the power input remains the same for Rule 1, it increases by several orders of magnitude for Rule 3. Thus, as seen above, it is better to use Rule 1 as we would be spending way too much energy for no additional improvement in product distribution if we use Rule 3.

Figures 13a and 13b show the application of the scale-up rules to the reaction system of Example II. The specifications of the laboratory-scale reactor are: configuration R1, $D = 0.5$ m, $N = 2.3355$ rps, $n_f = 1$, and $t_f = 1{,}800$ s. The reactions are very fast and we are barely into the micromixing controlled regime for the laboratory-scale reactor. Hence, we expect the product distribution to be sensitive to changes in the value of the mixing index with reactor size. Figure 13a shows the comparison of Rules 1 and 3. In this case the product distribution increases (becomes less favorable) with reactor size for Rule 1 as Q decreases while Da_m remains constant. For Rule 3, as the reactor size increases, both Q and Da_m decrease. The decrease in Da_m more than compensates for the decrease in Q, thus decreasing the product distribution. However, as for

the previous example, the power input per unit volume increases with increasing reactor size for Rule 3. Such an increase may be justified in this case as it improves the performance. If we cannot change the power input, similar benefits can be obtained from changing the feed addition time. Figure 13b shows a comparison of Rules 1 and 2. For Rule 2, the product distribution stays unaffected as both Q and Da_m remain unaffected. However, excessively long feed addition times are required at larger scales.

The scale-up rules are based on average flow properties. However, they are expected to be fairly accurate even when spatial variations of flow properties are taken into account. This is demonstrated in Figure 14, which shows the product distributions calculated by following Rules 1, 2, and 3 for the above example using the EFM for flow properties. Although the numerical values of the product distribution are different, trends similar to those in Figure 13 are observed.

Note that the appropriate heat-transfer equipment may be different at different scales as the heat-transfer surface area (A_s) and the reactor heat load (Q_G) change with scale in different ways. Step 3 of the synthesis procedure can easily be used to determine the appropriate heat-transfer equipment at any scale.

Conclusions

We have formulated a three-component development procedure for liquid-phase agitated reactors in specialty chemical processes. This procedure is shown in Figure 15. The first component is a three-step synthesis procedure. With information about the proposed reaction from a chemist and production plan from a business manager, a reactor which meets the desired performance is synthesized (Lerou and Ng, 1996). Although this method is based on the advances in the field of turbulent reactive mixing, it is in stark contrast to those fundamental analyses in which the reactor configuration is fixed.

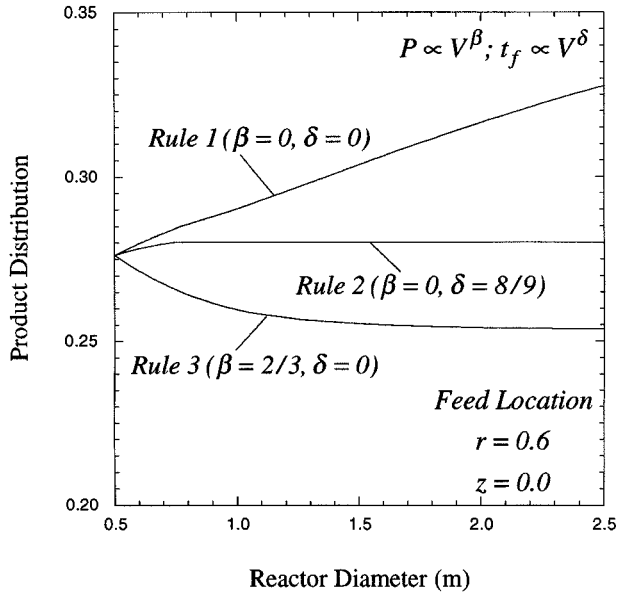

Figure 14. Effect of spatial variations of flow properties on product distribution upon scale-up.

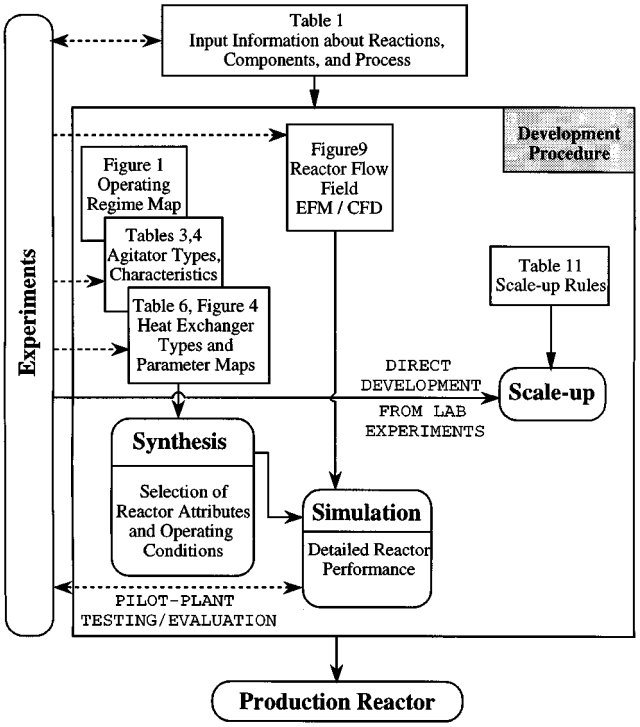

Figure 15. Procedure for development of agitated reactors for liquid-phase specialty chemicals processes.

Instead, the mixing index, and the Damköhler numbers for micro- and mesomixing that would meet performance objectives are identified without assuming a reactor design. Then, a reactor is aggregated from reactor attributes and operating conditions such as impeller type and speed, feed time, location, and number of feed ports that would yield those desired dimensionless numbers. Finally, heat-transfer equipment is added to the reactor thus assembled based on the heat-transfer requirement. At the early stage of process development, there is often a great deal of uncertainty about the reaction and the business plan. Due to its hierarchical nature, new information can be conveniently taken into account in this synthesis procedure as it becomes available. Also, the ability to manipulate the reactor attributes and the operating conditions allows greater flexibility in reactor design.

The second component rigorously evaluates the candidate reactor through simulations. The data on spatial variations of velocity and rate of turbulent energy dissipation per unit mass are obtained from experiments or CFD. This performance evaluation is particularly important if nonstandard impellers, baffles, reactor bottoms, additional reactor parts such as thermal wells and analytical instruments such as an *in-situ* FTIR may be present. This component is kept separate from the first component so as to reduce development time and cost and to allow greater flexibility for the synthesis task.

Due to the pressure of quick time-to-market, it is not unusual to scale up a laboratory reactor to a production-scale reactor. Our development procedure can be used to aid in this effort as follows. The synthesis component provides a candidate reactor with minimum effort. Then, the scale-up

component indicates, with justifications, how the operating conditions should be readjusted to at least preserve the performance objectives in the commercial reactor.

This article represents a part of our work on reaction system synthesis from a process systems engineering perspective. A similar approach has been used for multiphase reactors (Kelkar and Ng, 1998), precipitation reactors (Kelkar and Ng, 1999), liquid-liquid extractive reaction reactors (Samant and Ng, 1998a,b,c), and prepolymerization reactors (Samant and Ng, 1999). Further work on other reactor systems is underway.

Acknowledgments

Financial support from the National Environmental Technology Institute and the National Science Foundation (Grant No. 9807101) is gratefully acknowledged. We appreciate the many valuable interactions with our colleagues at G. D. Searle and Co. on this research. In particular, we thank Prabir Basu and Christine Seymour for their encouragement and guidance, without which this work would not have been possible.

Notation

a = ratio of feed volume to reactor volume
A_s^{ref} = reference heat transfer surface area, m^2
A, B, C, D, E = generic chemical species
C_p = specific heat capacity at constant pressure, J/kg·K
d = agitator diameter, m
D = reactor diameter, m
f = self-engulfment factor
h = clearance off tank bottom, m
H = reactor height, m
k_i = forward rate constant of reaction i, 1/s
$k_{\max}$ = largest forward rate constant in a reaction scheme, 1/s
n_b = number of agitator blades
N = agitator rotational speed, rps
N_{Nu} = Nusselt number
N_{Pr} = Prandtl number
N_{Re} = agitator Reynolds number
Q_G = reactor heat load, W
Q_R = heat-transfer capacity of heat-transfer equipment, W
R_i = rate of reaction i per mole of reaction mixture, 1/s
t_m = characteristic micromixing time, s
$\tilde{t}$ = average residence time for continuous operation, s
T = temperature, K
V = volume of micromixed fluid elements, m^3
V_R = reactor volume, m^3
w = agitator blade width, m
w_b = width of baffles, m
x_i = mole fraction of component i in the micromixed fluid elements
x_i^F = mole fraction of component i in the feed stream
y_i = mole fraction of component i in the environment
α = agitator pitch
λ = thermal conductivity, W/m·K
μ = viscosity, kg/m·s
ν = kinematic viscosity, m^2/s
θ = dimensionless time
ξ = ratio of agitator diameter to reactor diameter
ρ = density, kg/m^3
$\nu_{i,m}$ = stoichiometric coefficient of component i in reaction m
$\nu_{\text{TOT},m}$ = algebraic sum of the stoichiometric coefficients of the components in reaction, m

Subscripts

avg = average value
i, j = indices
min = minimum attainable value
max = maximum attainable value

Superscript

I, II = indices

Literature Cited

Baldyga, J., and J. R. Bourne, "A Fluid Mechanical Approach to Turbulent Mixing and Chemical Reaction: II. Micromixing in the Light of Turbulence Theory," *Chem. Eng. Commun.*, **28**, 243 (1984a).

Baldyga, J., and J. R. Bourne, "A Fluid Mechanical Approach to Turbulent Mixing and Chemical Reaction: III. Computational and Experimental Results for the New Micromixing Model," *Chem. Eng. Commun.*, **28**, 259 (1984b).

Baldyga, J., and S. Rohani, "Micromixing Described in Terms of Inertial-Convective Disintegration of Large Eddies and Viscous-Convective Interaction Among Small Eddies," *Chem. Eng. Sci.*, **42**, 2597 (1987).

Baldyga, J., and J. R. Bourne, "Micromixing in Inhomogeneous Turbulence," *Chem. Eng. Sci.*, **43**, 107 (1988).

Baldyga, J., and J. R. Bourne, "Simplification of Micromixing Calculations: I. Derivation and Application of New Model," *Chem. Eng. J.*, **42**, 83 (1989).

Baldyga, J., and J. R. Bourne, "Interaction Between Mixing on Various Scales in Stirred Tank Reactors," *Chem. Eng. Sci.*, **47**, 1839 (1992).

Baldyga, J., and R. Pohorecki, "Turbulent Micromixing in Chemical Reactors—A Review," *Chem. Eng. J.*, **58**, 183 (1995).

Baldyga, J., J. R. Bourne, and S. J. Hearn, "Interaction Between Chemical Reactions and Mixing on Various Scales," *Chem. Eng. Sci.*, **52**, 457 (1997).

Bates, R. L., P. L. Fondy, and J. G. Fenic, "Impeller Characteristics and Power," *Mixing: Theory and Practice Volume I*, V. M. Uhl and J. B. Gray, eds., Academic Press, New York (1966).

Biegler, L. T., I. E. Grossmann, and A. W. Westerberg, *Systematic Methods of Chemical Process Design*, Prentice Hall, Englewood Cliffs, NJ (1997).

Bolliger, D. H., "Assessing Heat Transfer in Process-Vessel Jackets," *The Chemical Engineering Guide to Heat Transfer: II. Equipment*, K. J. McNaughton, ed., McGraw-Hill, New York (1986).

Bondy, F., and S. Lippa, "Heat Transfer in Agitated Vessels," *The Chemical Engineering Guide to Heat Transfer: II. Equipment*, K. J. McNaughton, ed., McGraw-Hill, New York (1986).

Bourne, J. R., and P. Dell'Ava, "Micro- and Macro-Mixing in Stirred-Tank Reactors of Different Sizes," *Chem. Eng. Res. Des.*, **65**, 180 (1987).

Bourne, J. R., and C. P. Hilber, "The Productivity of Micromixing Controlled Reactions: Effect of Feed Distribution in Stirred Tanks," *Trans. IChemE.*, **68**, 51 (1990).

Bourne, J. R., and S. Yu, "Investigation of Micromixing in Stirred Tank Reactors Using Parallel Reactions," *Ind. Eng. Chem. Res.*, **33**, 41 (1994).

Chakrabarti, M., R. M. Kerr, and J. C. Hill, "Direct Numerical Simulation of Chemical Selectivity in Homogeneous Turbulence," *AIChE J.*, **41**, 2356 (1995).

Chella, R., and J. M. Ottino, "Conversion and Selectivity Modifications Due to Mixing in Unpremixed Reactors," *Chem. Eng. Sci.*, **39**, 551 (1984).

David, R., and J. Villermaux, "Interpretation of Micromixing Effects on Fast Consecutive-Competing Reactions in Semi-Batch Stirred Tanks by a Simple Interaction Model," *Chem. Eng. Commun.*, **54**, 333 (1987).

Douglas, J. M., *Conceptual Design of Chemical Processes*, McGraw-Hill, New York (1988).

Fasano, J. B., and W. R. Penney, "Cut Reaction By-Products by Proper Feed Blending," *Chem. Eng. Prog.*, **87**, 46 (1991).

Fort, I., "Flow and Turbulence in Vessels with Axial Impellers," *Mixing: Theory and Practice Volume III*, V. W. Uhl and J. B. Gray, eds., Academic Press, New York (1986).

Fox, R. O., "Computation of Turbulent Reactive Flows: First-Principles Macro/Micromixing Models Using Probability Density Function Methods," *Chem. Eng. Sci.*, **47**, 2853 (1992).

Kelkar, V. V., and K. M. Ng, "Screening Procedure for Synthesizing Isothermal Multiphase Reactors," *AIChE J.*, **44**, 1563 (1998).

Kelkar, V. V., and K. M. Ng, "Design of Reactive Crystallization Systems Incorporating Kinetics and Mass Transfer Effects," *AIChE J.*, **45**, 69 (1999).
Kresta, S. M., and P. E. Wood, "Prediction of the Three-Dimensional Turbulent Flow in Stirred Tanks," *AIChE J.*, **37**, 448 (1991).
Leonard, A. D., and J. C. Hill, "Direct Numerical Simulation of Turbulent Flows with Chemical Reaction," *J. Sci. Comput.*, **3**, 25 (1988).
Lerou, J. J., and K. M. Ng, "Chemical Reaction Engineering: A Multiscale Approach to a Multiobjective Task," *Chem. Eng. Sci.*, **51**, 1595 (1996).
Levenspiel, O., *Chemical Reaction Engineering*, 2nd ed., Wiley, New York (1972).
Mann, R., S. K. Pillai, A. M. El-Hamouz, P. Ying, A. Togatorop, and R. B. Edwards, "Computational Fluid Mixing for Stirred Vessels: Progress from Seeing to Believing," *Chem. Eng. J.*, **59**, 39 (1995).
Nagata, S., *Mixing: Principles and Applications*, Halstead Press, New York (1975).
Oldshue, J. Y., *Fluid Mixing Technology*, McGraw-Hill, New York (1983).
Ottino, J. M., "Efficiency of Mixing from Data on Fast Reactions in Multi-Jet Reactors and Stirred Tanks," *AIChE J.*, **27**, 184 (1981).
Paul, E. L., and R. E. Treybal, "Mixing and Product Distribution for a Liquid-Phase, Second-Order, Competitive-Consecutive Reaction," *AIChE J.*, **17**, 718 (1971).
Paul, E. L., "Design of Reaction Systems for Specialty Organic Chemicals," *Chem. Eng. Sci.*, **43**, 1773 (1988).
Paul, E. L., M. Mahadevan, J. Foster, M. Kennedy, and M. Midler, "The Effect of Mixing on Scale-up of a Parallel Reaction System," *Chem. Eng. Sci.*, **47**, 2837 (1992).
Pipino, M., and R. O. Fox, "Reactive Mixing in a Turbular Jet Reactor: A Comparison of PDF Simulations with Experimental Data," *Chem. Eng. Sci.*, **49**, 5229 (1994).
Ranade, V. V., and J. B. Joshi, "Flow Generated by Pitched-Blade Turbines: I. Measurements Using Laser Doppler Anemometer," *Chem. Eng. Commun.*, **81**, 197 (1989).
Ranade, V. V., J. B. Joshi, and A. G. Marathe, "Flow Generated by Pitched-Blade Turbines: II. Simulation Using k-ϵ Model," *Chem. Eng. Commun.*, **81**, 225 (1989).
Ranade, V. V., and J. B. Joshi, "Flow Generated by a Disc Turbine: I. Experimental," *Trans. IChemE.*, **68**(A), 19 (1990a).
Ranade, V. V., and J. B. Joshi, "Flow Generated by a Disc Turbine: II. Mathematical Modeling and Comparison with Experimental Data," *Trans. IChemE.*, **68**(A), 34 (1990b).
Ranade, V. V., "Computational Fluid Dynamics for Reactor Engineering," *Reviews in Chem. Eng.*, **11**, 229 (1995).
Samant, K. D., and K. M. Ng, "Synthesis of Extractive Reaction Processes," *AIChE J.*, **44**, 1363 (1998a).
Samant, K. D., and K. M. Ng, "Effect of Kinetics and Mass Transfer on Design of Extractive Reaction Processes," *AIChE J.*, **44**, 2212 (1998b).
Samant, K. D., and K. M. Ng, "Design of Multistage Extractive Reaction Processes," *AIChE J.*, **44**, 2689 (1998c).
Samant, K. D., and K. M. Ng, "Synthesis of Prepolymerization Stage in Polycondensation Processes," *AIChE J.*, **45**, 1808 (1999).
Sano, Y., and H. Usui, "Interrelations among Mixing Time, Power Number, and Discharge Flow Rate Number in Baffled Mixing Vessels," *J. Chem. Eng. Japan*, **18**, 47 (1985).
Schafer, M., M. Yianneskis, P. Wachter, and F. Durst, "Trailing Vortices around a 45° Pitched-Blade Impeller," *AIChE J.*, **44**, 1233 (1998).
Shah, Y. T., "Design Parameters for Mechanically Agitated Reactors," *Adv. in Chem. Eng.*, **17**, 1 (1991).
Tatterson, G. B., *Fluid Mixing and Gas Dispersion in Agitated Tanks*, McGraw-Hill, New York (1991).
Tipnis, S. K., W. R. Penney, and J. B. Fasano, "An Experimental Investigation to Determine a Scale-up Method for Fast Competitive Parallel Reactions in Agitated Vessels," *Ind. Mixing Technology: Chemical and Biological Applications*, G. B. Tatterson, R. V. Calabrese, and W. R. Penney, eds., AIChE Symp. Ser., **90**(299), AIChE, New York (1994).
Toor, H. L., "Mass Transfer in Dilute Turbulent and Nonturbulent Systems with Rapid Irreversible Reactions and Equal Diffusivities," *AIChE J.*, **8**, 70 (1962).
Toor, H. L., "Turbulent Mixing of Two Species with and without Chemical Reactions," *Ind. Eng. Chem. Fundam.*, **8**, 655 (1969).
Uhl, V. W., "Mechanically Aided Heat Transfer," *Mixing: Theory and Practice: I.*, V. W. Uhl and J. B. Gray, eds., Academic Press, New York (1966).
Villermaux, J., and L. Falk, "A Generalized Mixing Model for Initial Contacting of Reactive Fluids," *Chem. Eng. Sci.*, **49**, 5127 (1994).
Wu, H., and G. K. Patterson, "Laser Doppler Measurements of Turbulent Flow Parameters in a Stirred Mixer," *Chem. Eng. Sci.*, **44**, 2207 (1989).
Zlokarnik, M., and H. Judat, "Stirring," *Ullmann's Encyclopedia of Industrial Chemistry*, 5th ed., Vol. B2, p. 25-1 (1988).

Appendix: Engulfment Model in Mole Fraction Space

Traditionally, the phenomenological model equations for micromixing have been developed in the composition space (Baldyga and Bourne, 1984a,b, 1989). However, it is much more convenient to classify the reactor operation into various operating regimes if these equations are written in the mole fraction space. The engulfment model equations can be written in the mole fraction space as described here.

In the engulfment model, the balance equations for the growing fluid elements are

$$\frac{dV}{dt} = EVf \tag{A1a}$$

$$\frac{dN_i}{dt} = \langle c_i \rangle \frac{dV}{dt} + N_T \sum_{j=1}^{r} \nu_{i,j} R_j \tag{A1b}$$

N_i and N_T are the number of moles of component i and total number of moles, respectively, in the growing fluid elements. $\langle c_i \rangle$ is the concentration of component i in the environment. All other terms have their usual meanings. A summation of Eq. A1b over all components gives

$$\frac{dN_T}{dt} = \left(\sum_{i=1}^{c} \langle c_i \rangle \right) \frac{dV}{dt} + N_T \sum_{j=1}^{r} \nu_{\mathrm{TOT},j} R_j \tag{A2}$$

Also, by differentiating $x_i = N_i/N_T$, we get,

$$\frac{dx_i}{dt} = \frac{1}{N_T} \frac{dN_i}{dt} - \frac{x_i}{N_T} \frac{dN_T}{dt} \tag{A3}$$

Substituting Eqs. A1b and A2 into Eq. A3, we get

$$\frac{dx_i}{dt} = \left[\frac{\langle c_i \rangle}{N_T} - \frac{x_i \sum_{i=1}^{c} \langle c_i \rangle}{N_T} \right] \frac{dV}{dt} + \sum_{j=1}^{r} (\nu_{i,j} - x_i \nu_{\mathrm{TOT},j}) R_j \tag{A4}$$

By using Eq. A1a, $N_T = V \sum_{i=1}^{c} c_i$, and $y_i = \langle c_i \rangle / \sum_{i=1}^{c} \langle c_i \rangle$, the first term on the righthand side of Eq. A4 can be written as

$$\left[\frac{\langle c_i \rangle}{N_T} - \frac{x_i \sum_{i=1}^{c} \langle c_i \rangle}{N_T} \right] EVf = \frac{\sum_{i=1}^{c} \langle c_i \rangle}{\sum_{i=1}^{c} c_i} [y_i - x_i] Ef \tag{A5}$$

Here, the concentration terms are

$$\sum_{i=1}^{c} c_i = \rho_x / M_x \tag{A6a}$$

$$\sum_{i=1}^{c} \langle c_i \rangle = \rho_y / M_y \tag{A6b}$$

It is reasonable to assume the mass density of the single-phase liquid mixture to be constant irrespective of its composition. Hence, we get

$$\rho_x = \rho_y$$

$$\frac{\sum_{i=1}^{c} \langle c_i \rangle}{\sum_{i=1}^{c} c_i} = \frac{M_x}{M_y} \tag{A7}$$

Using the above developments, we get

$$\frac{dx_i}{dt} = \frac{M_x}{M_y}(y_i - x_i) Ef + \sum_{j=1}^{r} (\nu_{i,j} - x_i \nu_{\mathrm{TOT},j}) R_j \tag{A8}$$

Substituting for E (Eq. 3) and f (Eq. 5), we get

$$\frac{dx_i}{dt} = \frac{1}{t_m}\frac{M_x}{M_y}(y_i - x_i)\left[1 - \frac{V}{V_o}\exp\left(\frac{-t}{t_s}\right)\right] + \sum_{j=1}^{r} (\nu_{i,j} - x_i \nu_{\mathrm{TOT},j}) R_j \tag{A9}$$

The initial condition, of course, is

$$x_i(t=0) = x_i^F \tag{A10}$$

Manuscript received Mar. 8, 1999, and revision received Aug. 6, 1999.